

Exponential Conic Optimization for Multi-Regime Service System Design under Congestion and Tail-Risk Control

Víctor Blanco[†], Miguel Martínez-Antón[‡], and Justo Puerto[‡]

[†]Institute of Mathematics (IMAG), Universidad de Granada

vblanco@ugr.es

[‡]Institute of Mathematics (IMUS), Universidad de Sevilla

mmartinez31@us.es, puerto@us.es

ABSTRACT. We study the design of single-facility service systems operating under multiple recurring regimes with service-level constraints on response times. Regime-dependent arrival and service rates induce hyperexponential response-time distributions, and the design problem selects regime-specific capacities to balance cost, congestion, fairness, and reliability. We propose a mixed-integer exponential conic optimization framework integrating SLA chance constraints, conflict-graph design restrictions, and CVaR-based tail-risk control. Although NP-hard, the problem admits an efficient decomposition scheme and tractable special cases. Computational experiments and a large-scale urban case study show substantial improvements over the current system, quantifying explicit trade-offs between efficiency, congestion control, fairness, and robustness. The framework provides a practical tool for congestion-aware and tail-control service system design.

1. INTRODUCTION

Service systems in both private and public sectors increasingly operate under explicit performance requirements that regulate not only average congestion levels but also the reliability of user response times. Such requirements arise in customer support operations, logistics and transportation services, emergency response systems, healthcare delivery, and cloud computing infrastructures. Service-level agreement (SLA), in these contexts, typically imposes probabilistic guarantees, requiring congestion-induced delays to remain below prescribed thresholds with high confidence. Designing service systems that satisfy reliability requirements at minimum operational cost is therefore a central problem in operations research.

A defining feature of modern service systems is demand heterogeneity. Demand elements differ in their exogenous access characteristics, such as network latency, travel time, or dispatch delay, while sharing access to capacity-constrained service resources. Accordingly, a user's total response time model naturally decomposes into a deterministic access component and a stochastic congestion component arising from waiting and service at the facility. Meaningful reliability guarantees must therefore account for heterogeneous demand rather than relying solely on aggregate averages.

In addition, real systems rarely operate as a single homogeneous queue. Instead, service capacity is often structured into a certain number of recurring operating regimes that differ systematically in congestion conditions and processing speed. These regimes may represent alternative staffing configurations, distinct service modes, specialized resources, or routing

policies. Examples include differentiated support tiers, parallel processing pipelines in cloud systems, fast and slow treatment tracks in healthcare, and multiple dispatch channels in emergency response. Each regime behaves as a stable queueing system with its own arrival intensity and service capacity.

We model such systems as collections of parallel M/M/1 queues with regime-dependent arrival rates and service capacities, where incoming demand is probabilistically routed across regimes. Conditional on the selected regime, response times follow the classical exponential behavior of stable queues. However, from the perspective of an arbitrary arrival, regime assignment is random, and the overall response-time distribution becomes a mixture of exponential components. This hyperexponential structure arises endogenously from regime-based routing and captures the empirically observed coexistence of typical performance and occasional congestion episodes. At the same time, it preserves analytical tractability, admitting closed-form expressions for cumulative probabilities and expectations.

The goal of this paper is to exploit this structure for service system design. We develop a flexible optimization framework in which regime-specific service rates and routing-induced response-time distributions are decision variables. SLA enforcement is modeled selectively: binary activation variables determine which demand elements are protected by probabilistic response-time guarantees, while coverage and fairness requirements are imposed through additional constraints. Beyond individual SLA compliance, the framework incorporates explicit control of tail performance through convex risk measures, allowing the decision-maker to limit the average response time experienced by the worst-performing fraction of demand. This provides protection against extreme degradation without imposing overly conservative worst-case guarantees.

All these features are embedded in a unified mixed-integer conic optimization formulation that leverages the analytical structure of exponential queues. Exact expressions for response-time distributions lead to constraints that are representable with exponential cones, yielding tractable models that jointly enforce stability, selective SLA, congestion-sensitive loss functions, and tail-risk control. We show that the general design problem is NP-hard, while identifying structured special cases, such as uniform service-level confidence parameters, admitting polynomial-time solution procedures.

The contribution of this paper is thus a unified optimization framework for the reliability-oriented design of regime-based Poisson service systems. By integrating hyperexponential response-time structure, selective SLA coverage, and risk-aware performance criteria within an exponential cone-representable formulation, the proposed approach provides both theoretical insight and implementable decision-support tools. Computational experiments illustrate the trade-offs between capacity investment, congestion, and service reliability across alternative design paradigms.

1.1. Related Work. This paper relates to several streams of the operations research literature on queueing system design, service-level guarantees, and risk-aware optimization. Our emphasis is on optimization-based approaches that explicitly embed queueing performance measures into system design decisions.

Queueing theory form the backbone of service system analysis, capturing both capacity limitations and the temporal interaction between arrivals and service completions. Classical models such as M/M/1 and M/D/1 yield tractable expressions for key performance measures and underpin a large body of work on staffing, capacity planning, and control [Gross et al., 2008]. However, empirical evidence consistently points to substantial heterogeneity

and variability in service times, often leading to heavy-tailed or multimodal response-time distributions that are poorly approximated by single exponential models [Hokstad, 1978].

Hyperexponential and, even generally, phase-type distributions address this limitation by representing service times as mixtures of exponential regimes. These models have been widely used in telecommunications, computer systems, and cloud infrastructures to capture bursty behavior and rare congestion events [Asmussen, 2003, Feldmann and Whitt, 1998]. Despite their analytical tractability, hyperexponential models have been used primarily for performance evaluation, with relatively limited attention devoted to their systematic integration into optimization-based design frameworks.

Optimization models for service system design have a long tradition, particularly in call centers and service operations. Early and recent contributions study how staffing levels, service rates, and routing policies can be optimized to balance operating costs and delay-related performance measures [Borst et al., 2004, Garnett et al., 2002, Gómez and Anjos, 2017, Gurvich and Whitt, 2009, Harrison and Zeevi, 2005, Hassin and Haviv, 2003, Long et al., 2024, Tsitsiklis and Xu, 2017, Zychlinski et al., 2023]. These works typically rely on exponential service-time assumptions, diffusion approximations, or asymptotic regimes, and they often focus on average delays or probabilities of delay. In contrast, the explicit optimization of regime-dependent parameters in hyperexponential queueing systems, especially under tail-sensitive performance criteria, remains relatively uncharted.

Several works have also analyzed service network design and location problems under congestion effects, explicitly incorporating queueing performance into spatial decision models. Early contributions such as [Berman et al., 1985] study optimal server location on networks operating as $M/G/1$ queues, embedding waiting-time considerations into location decisions. Subsequent research has developed broader location frameworks with congestion, including models that account for interaction between spatial demand allocation and service delays [Berman et al., 2003], as well as location-allocation problems on congested networks [Aboolian et al., 2008]. More recent contributions consider probabilistic covering formulations under congestion [Aboolian et al., 2022a] and integrated service system design models with stochastic demand, congestion, and consumer choice [Aboolian et al., 2022b]. While these studies incorporate congestion into location decisions, they typically rely on steady-state queueing metrics or average-delay approximations. In contrast, our approach embeds exact regime-dependent response-time distributions directly into the design problem and explicitly controls reliability and tail performance through risk-sensitive optimization.

Service-level agreement provides a formal mechanism to encode performance requirements in many application domains, including telecommunications, cloud computing, logistics, and healthcare [Harchol-Balter, 2013, Jain et al., 2002]. In queueing-based optimization models, SLA is commonly imposed as probabilistic constraints on response times or as constraints on the fraction of customers served within a target time window [Cheng and Huo, 2013, Soh and Gurvich, 2017]. Most existing approaches enforce these constraints uniformly across all demand classes and rely on approximations or heuristics to maintain tractability.

Recent work has begun to relax uniformity assumptions by allowing selective or prioritized service guarantees, motivated by heterogeneity in demand value or delay sensitivity and differentiated service menus [Bertsimas et al., 2018, Caldentey et al., 2025, Daskin, 2013]. Nevertheless, such approaches are rarely combined with explicit continuous-time queueing dynamics and response-time chance constraints.

Tail-risk control has also received growing attention in optimization, notably through coherent risk measures as conditional value-at-risk (CVaR) [Rockafellar and Uryasev, 2000, 2002]. CVaR-based formulations admit tractable convex representations and have been successfully

applied in finance [Cesarone and Puerto, 2025], supply chain management, and network design [Ogryczak and Tamir, 2003, Puerto et al., 2017]. Their application to queueing system design remains limited, and prior works typically address worst-case or average performance rather than directly regulating the distribution of response times across users.

Finally, recent advances in conic optimization have enabled exact convex representations of nonlinear performance measures and risk constraints. Exponential cone formulations, in particular, allow logarithmic and exponential relationships to be embedded directly into optimization models [Ben-Tal and Nemirovski, 2001, Boyd and Vandenberghe, 2004, Chares, 2009]. While these tools have been exploited in congestion control and robust optimization, their potential for queueing system design with explicit response-time distributions has not been fully unraveled.

The present paper contributes to this literature by developing a unified optimization framework that integrates hyperexponential queueing structure, selective SLA enforcement, congestion-sensitive cost modeling, and CVaR-based tail-risk control within a single conic formulation. Unlike existing approaches, regime-dependent service capacities are treated as endogenous design variables, exact response-time expressions are embedded through exponential cones, and coverage and tail-risk characteristics can be tailored without altering the underlying model structure.

1.2. Contributions and Organization. This paper develops an optimization framework for the design of reliability-oriented service systems operating under multiple regimes. Rather than focusing on congestion evaluation, we embed the exact response-time structure of regime-based queues directly into capacity-design decisions, enabling explicit control of coverage, reliability, and tail risk.

Our contributions are fourfold. First, we model regime-dependent response-time distributions explicitly and treat service reliability and tail performance as primary design objectives, moving beyond average-delay or steady-state analyses. Second, we introduce endogenous selective service-level agreement, allowing the protected demand set to be determined within the optimization. Third, we incorporate CVaR-type tail control directly on response times and show that the resulting design problems admit exact mixed-integer exponential cone formulations. Fourth, we analyze the computational complexity of the model, prove its NP-hardness, and derive a polynomial-time algorithm for relevant cases. Together, these results yield a unified and tractable framework that transparently captures trade-offs between capacity investment, congestion, coverage, and extreme-delay protection.

The remainder of the paper is organized as follows. Section 2 derives the regime-based response-time expressions, characterizing the exact distributional structure induced by multiple operating regimes and establishing the analytical foundations that support the subsequent design models. Section 3 introduces the optimization framework, formulates the reliability-oriented capacity design problems, establishes their NP-hardness, and identifies relevant special cases that admit polynomial-time solution algorithms. Section 4 presents a detailed computational study based on a New York City EMS case study, illustrating the tractability of the proposed mixed-integer exponential conic formulations and quantifying the trade-offs between capacity investment, congestion, coverage, and tail-risk protection. Finally, Section 5 concludes the paper by summarizing the main findings, discussing managerial implications, and outlining promising directions for future research.

2. PERFORMANCE STRUCTURE OF MULTI-REGIME PARALLEL SERVICE SYSTEMS

We consider a service system motivated by a wide range of management science and operations research applications, including facility location, emergency response systems, centralized service centers, and capacity planning under uncertainty. Demand originates from a finite set of points \mathcal{A} , representing geographic zones, customer segments, or origin locations in a network. Service is provided through a finite collection of service regimes indexed by $\mathcal{R} := \{1, \dots, R\}$.

Each regime represents an independent service channel, operating as an M/M/1 queue with its own congestion characteristics. Customers are assigned to exactly one regime *prior to entering any queue*, and all waiting and service experienced by a customer take place exclusively within the queue associated with the selected regime. Therefore, regimes do not represent time-varying operating states of a single server, but rather parallel service channels that co-exist simultaneously. This modeling structure arises naturally in many service settings where demand is pre-classified or routed before processing. Examples include customer support systems with distinct service tiers or specialized teams, healthcare operations where patients are triaged into separate treatment tracks, cloud computing platforms that route requests to different processing pipelines, and emergency response systems where incidents are dispatched to alternative resources based on location or severity. In all these cases, customers commit to a specific service channel before experiencing congestion, and performance is governed by the load and capacity of the selected channel rather than by time-varying system states.

For each demand point $a \in \mathcal{A}$ and each service regime $r \in \mathcal{R}$, customers originating from a and routed to regime r arrive according to an independent Poisson process with rate $\lambda_{ar} \geq 0$. These arrival processes are assumed independent across demand points and regimes. The total arrival rate associated with demand point a is $\lambda_a := \sum_{r \in \mathcal{R}} \lambda_{ar}$, while the aggregate arrival rate to regime r is $\Lambda_r := \sum_{a \in \mathcal{A}} \lambda_{ar}$.

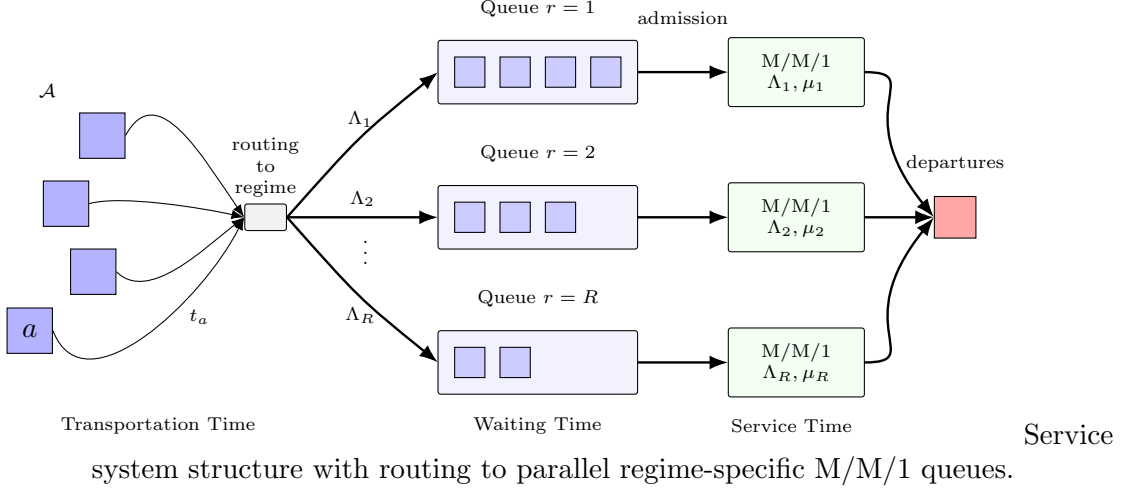
By the superposition property of Poisson processes, arrivals to each regime form a Poisson process with rate Λ_r . This viewpoint allows the composition of service regimes to vary across demand points and captures heterogeneity in routing patterns and service requirements.

The effective arrival rates $(\Lambda_r)_{r \in \mathcal{R}}$ depend on how demand is distributed across operating regimes. From a practical standpoint, the proposed methodology is deliberately flexible and can accommodate different system architectures, routing mechanisms, and levels of operational control. Let each demand point $a \in \mathcal{A}$ generate an exogenous demand rate $\lambda_a \geq 0$. In applied settings, the following arrival rate structures naturally arise.

We consider a regime-based structure in which the system operates under regime $r \in \mathcal{R}$ with probability $\pi_r \geq 0$, where $\sum_{r \in \mathcal{R}} \pi_r = 1$. In this setting, regime r receives an arrival inflow $\Lambda_r = \pi_r \sum_{a \in \mathcal{A}} \lambda_a$, so that the overall arrival rate $\Lambda := \sum_{a \in \mathcal{A}} \lambda_a$ is proportionally distributed across regimes according to the regime probabilities.

This formulation captures environments in which regimes represent recurring operational conditions—such as peak and off-peak periods, staffing configurations, or congestion states—rather than user-dependent routing policies. Each regime therefore corresponds to a distinct service configuration, and the overall response-time distribution arises as a mixture of regime-specific performance measures weighted by π_r .

Each arriving customer must first complete a deterministic transportation or access phase before entering the service system. For a customer originating at demand point a , this transportation time is denoted by $t_a \geq 0$ and is assumed to be known. This component captures physical travel time, communication latency, or any other exogenous delay that is independent



of congestion at the service regimes. Transportation time contributes additively to the total response time but does not affect the queueing dynamics within the service system.

Upon completion of transportation, each customer is routed to exactly one service regime r according to the routing structure encoded by the rates λ_{ar} . The customer then joins the corresponding queue, which operates under a first-come, first-served discipline with unlimited waiting space. Conditional on regime r , service times are exponentially distributed with rate $\mu_r > 0$. Thus, regime r behaves as a stable M/M/1 queue provided that $\Lambda_r < \mu_r$.

Figure ?? illustrates the system structure. Customers originate at demand points, incur deterministic transportation times, are routed to one of the service regimes, and then experience waiting and service according to the congestion level of the selected regime. For each regime $r \in \mathcal{R}$, the utilization factor is $0 \leq \rho_r := \frac{\Lambda_r}{\mu_r} < 1$. Under regime r , an arriving customer enters service immediately with probability $1 - \rho_r$ and experiences a positive waiting time with probability ρ_r .

The following result states the distribution of the total response time of the system for each demand point $a \in \mathcal{A}$.

Theorem 1. *The total (end-to-end) response time R_a of the system for a demand point $a \in \mathcal{A}$ follows a shifted hyperexponential with cumulative distribution function*

$$\mathbb{P}(R_a \leq t) = \begin{cases} 0 & \text{if } t < t_a, \\ 1 - \sum_{r \in \mathcal{R}} \pi_r e^{-(\mu_r - \Lambda_r)(t - t_a)} & \text{if } t \geq t_a, \end{cases}$$

and expectation

$$\mathbb{E}[R_a] = t_a + \sum_{r \in \mathcal{R}} \frac{\pi_r}{\mu_r - \Lambda_r},$$

where mixture weights $\pi_r := \frac{\Lambda_r}{\sum_{r' \in \mathcal{R}} \Lambda_{r'}}$ for all $r \in \mathcal{R}$.

Proof. Proof. A classical result for the M/M/1 queue implies that, conditional on regime r , the stationary sojourn time at the facility, defined as the sum of the waiting and service times, is exponentially distributed with rate $\mu_r - \Lambda_r$ [see, e.g., Kleinrock, 1975, Wolff, 1989]. Since

an arbitrary arrival is routed to regime r with probability

$$\pi_r = \frac{\Lambda_r}{\sum_{r' \in \mathcal{R}} \Lambda_{r'}},$$

the unconditional sojourn time T of a random demand point follows a hyperexponential distribution with mixture weights π_r and exponential rates $\mu_r - \Lambda_r$. Therefore, it follows that the cumulative distribution function of T is

$$\mathbb{P}(T \leq t) = 1 - \sum_{r \in \mathcal{R}} \pi_r e^{-(\mu_r - \Lambda_r)t} \quad \text{if } t \geq 0,$$

and 0 otherwise; and its expectation is $\mathbb{E}[T] = \sum_{r \in \mathcal{R}} \frac{\pi_r}{\mu_r - \Lambda_r}$.

Finally, the total response time model of the system is defined as the sum of the deterministic transportation time plus the stochastic sojourn time ($R_a = t_a + T$). Since the transportation time t_a is deterministic, the claim follows from shifting by t_a the cumulative distribution function and the expectation of T . \square

In particular, the dependence of $\mathbb{E}[R_a]$ on a arises exclusively through the transportation time, t_a , while congestion effects are captured by the regime-level service slack $\mu_r - \Lambda_r$ and the routing weights π_r .

This performance structure makes explicit how demand-specific arrival rates (λ_{ar}), service capacities (μ_r), and transportation times (t_a) jointly determine congestion and response-time distributions. The resulting closed-form expressions for utilization and response-time probabilities provide a rigorous and tractable foundation for optimization models that balance efficiency, equity, and risk in regime-structured service system design.

Service-level agreement imposes probabilistic performance guarantees on the total response time experienced by demand elements. For every demand $a \in \mathcal{A}$, fix a tolerance level $\alpha_a \in [0, 1]$ and a response-time threshold $t_a^* \geq t_a$. The SLA requirement for element a is expressed as a chance constraint of the form

$$\mathbb{P}(R_a \leq t_a^*) \geq 1 - \alpha_a, \tag{1}$$

which enforces that the response-time target is met with high probability.

Corollary 1. *Let $a \in \mathcal{A}$ be a demand point. Given a tolerance level $0 \leq \alpha_a \leq 1$ and a total response time threshold $t_a^* \geq t_a$ for a , the corresponding SLA requirement (1) of the system admits an explicit representation as*

$$\sum_{r \in \mathcal{R}} \pi_r e^{-(\mu_r - \Lambda_r)(t_a^* - t_a)} \leq \alpha_a. \tag{2}$$

Proof. Proof. The result is a direct consequence of Theorem 1. \square

Note that the left-hand side in (2) captures the contribution of each service regime to the tail probability of excessive delay.

In the case of a single regime, $|\mathcal{R}| = 1$, the expression (2) simplifies to the following lower bound for the service rate of the queue

$$\mu_1 \geq \Lambda_1 - \frac{\log(\alpha_a)}{t_a^* - t_a}. \tag{3}$$

In many practical settings, such guarantees are not required uniformly across the entire demand population. Instead, service-level agreement is enforced only for a selected subset of demand elements, reflecting contractual obligations, regulatory requirements, or prioritization policies. Let $S \subseteq \mathcal{A}$ denote the set of demand points for which the SLA condition (1) is

imposed, while no probabilistic guarantee is required for elements in $\mathcal{A} \setminus S$. This selective enforcement mechanism plays a central role in the design framework developed in the next section, where the protected set S is determined endogenously as part of the optimization process.

Remark 1. *The framework developed in this paper exploits the analytical structure induced by Poisson arrivals and exponential service within each regime, which yields closed-form expressions for response-time distributions and enables compact exponential cone representations of stability, service-level, and tail-risk constraints. This choice is motivated by tractability and by the fact that exponential service provides the simplest setting in which congestion and routing-induced variability interact.*

The approach extends naturally to regimes with Erlang- k service times. In this case, each regime remains an M/G/1 queue, expected waiting and sojourn times follow from standard Pollaczek–Khinchine results, and the sojourn-time distribution admits a phase-type representation that can be expressed as a finite combination of exponential and polynomial–exponential terms [see, e.g., [Asmussen, 2003](#), [Gross et al., 2008](#)]. While the resulting constraints are algebraically more involved, they preserve the essential structure required for convex and conic optimization. Accordingly, the exponential-service assumption should be viewed as a modeling choice rather than a limitation.

The design problems studied in this paper are formulated as optimization models that explicitly exploit the analytical structure of the response-time distributions derived above. In particular, the probabilistic service-level constraints and congestion-sensitive cost terms involve exponential and logarithmic relationships that arise naturally from the hyperexponential sojourn-time expressions. These relationships are represented exactly using exponential cone programming. The exponential cone $\mathcal{K}_{\text{exp}} \subset \mathbb{R}^3$ is defined as

$$\mathcal{K}_{\text{exp}} := \left\{ (x, y, z) \in \mathbb{R}^3 : x \geq y e^{z/y}, y > 0 \right\} \cup \left\{ (x, 0, z) \in \mathbb{R}^3 : z \leq 0 \leq x \right\},$$

which is a proper cone that provides an exact conic representation of exponential and logarithmic inequalities. Its dual cone is given by

$$\mathcal{K}_{\text{exp}}^* = \left\{ (u, v, w) \in \mathbb{R}^3 : eu \geq -we^{v/w}, w < 0 \right\} \cup \left\{ (u, v, 0) : u, v \geq 0 \right\}.$$

Within this framework, the service system design problem is expressed using linear constraints, exponential cone constraints, and a limited number of integer restrictions. Continuous decision variables encode quantities such as service rates, congestion margins, and auxiliary variables associated with response-time bounds, whereas binary variables are used to model the selective activation of service-level guarantees. Optimization models of this nature belong to the class of mixed-integer exponential cone programs, which generalize mixed-integer linear programming by allowing exponential relationships to be represented without approximation. Modern conic optimization solvers, as [Mosek \[2025\]](#), support \mathcal{K}_{exp} directly, enabling the exact and tractable integration of queueing-based performance constraints, stability conditions, and tail-risk controls into a unified optimization model.

3. DESIGN FRAMEWORK AND OPTIMIZATION MODEL

This section introduces a unified optimization framework for the design of a multi-regime parallel service system under a conflict-aware reliable service coverage, concerned about cost-congestion tradeoffs and least-favored users' tail care. The framework supports the joint

selection of regime-dependent service capacities and the service quality-driven protected segment of the demand population. These decisions are made while explicitly enforcing stability conditions and controlling response-time reliability, and tail-risk performance at the population level.

Decision Variables

In what follows, we describe the decision variables used in our model.

- **Service rates.** The primary design variables are the regime-dependent service rates μ_r , $r \in \mathcal{R}$, which represent staffing levels, server speeds, or effective processing capacities assigned to each service regime. These variables directly determine congestion through the service slack $\mu_r - \Lambda_r$ and therefore govern both expected response times and tail performance.
- **SLA-protected set.** To model the selective enforcement of service-level agreement, we introduce binary activation variables $s_a \in \{0, 1\}$ for each demand point $a \in \mathcal{A}$. The value $s_a = 1$ indicates that demand point a belongs to the protected set $S \subseteq \mathcal{A}$ for which probabilistic response-time guarantees are imposed, whereas $s_a = 0$ points out that no SLA constraint is required for that element.

Feasibility Requirements

Feasibility requires stability in every service regime and satisfaction of the service-level constraints for the protected set S . In what follows, we describe how these conditions are modeled in our formulation.

- **Stability.** This mandatory condition is enforced through a strict slack condition ensuring the utilization factor in each regime, ρ_r , is strictly under 1,

$$\mu_r - \Lambda_r \geq \varepsilon, \quad \forall r \in \mathcal{R}, \quad (4)$$

where $\varepsilon > 0$ is a small numerical parameter chosen consistently with solver tolerances. This condition guarantees that each regime operates in a stable M/M/1 regime and avoids numerical issues associated with boundary solutions.

- **Selective SLA enforcement.** Let t_a^* denote the response-time threshold for demand point a and let $\alpha_a \in [0, 1]$ denote its admissible violation probability. To enforce the SLA condition (1) only when $s_a = 1$, we show the following result.

Lemma 1. *Let $\zeta_{ar} \geq 0$ be nonnegative auxiliary variables for $a \in \mathcal{A}$ and $r \in \mathcal{R}$. The following set of mixed-integer exponential cone constraints,*

$$\sum_{r \in \mathcal{R}} \pi_r \zeta_{ar} \leq 1 + (\alpha_a - 1)s_a, \quad (5)$$

$$(\zeta_{ar}, s_a, -(\mu_r - \Lambda_r)(t_a^* - t_a)) \in \mathcal{K}_{\text{exp}}, \quad (6)$$

for all $a \in \mathcal{A}$ and $r \in \mathcal{R}$, ensures the SLA (1) is just required for the elements of $S := \{a \in \mathcal{A} : s_a = 1\}$ in the system.

In the single regimen case, $|\mathcal{R}| = 1$, the stability (4) and SLA enforcement (5)-(6) can be compactly simplified to

$$\mu_1 \geq \left(\max \left\{ \varepsilon, -\frac{\log(\alpha_a)}{t_a^* - t_a} \right\} - \varepsilon \right) s_a + \Lambda_1 + \varepsilon, \quad \forall a \in \mathcal{A}.$$

Proof. Suppose first that $a \notin S$, then $s_a = 0$. Hence, constraint (6) becomes

$$(\zeta_{ar}, 0, -(\mu_r - \Lambda_r)(t_a^* - t_a)) \in \mathcal{K}_{\text{exp}}, \quad \forall r \in \mathcal{R}$$

which is trivially verified by nonnegativity of ζ_{ar} and nonpositivity of $-(\mu_r - \Lambda_r)(t_a^* - t_a)$, where this latter is due to the stability condition (4). Therefore, constraint (5), which reduces to $\sum_{r \in \mathcal{R}} \pi_r \zeta_{ar} \leq 1$, becomes nonbinding. Thus, no condition is imposed to demand a . Otherwise, if $a \in S$, then $s_a = 1$. Hence, constraint (6) becomes

$$e^{-(\mu_r - \Lambda_r)(t_a^* - t_a)} \leq \zeta_{ar}, \quad \forall r \in \mathcal{R}$$

and constraint (5) reduces to $\sum_{r \in \mathcal{R}} \pi_r \zeta_{ar} \leq \alpha_a$, what together implies that

$$\alpha_a \geq \sum_{r \in \mathcal{R}} \pi_r \zeta_{ar} \geq \sum_{r \in \mathcal{R}} \pi_r e^{-(\mu_r - \Lambda_r)(t_a^* - t_a)}.$$

Then, (2) holds. Thus, by Corollary 1, SLA condition (1) also holds for a .

For the case $|\mathcal{R}| = 1$, the result follows straightforward by the observation in (3). \square

Apart from stability and selective SLA enforcement, no additional feasibility requirements are imposed in the base model. Note that in such base model the best decision is set $s_a = 0$ for all demand $a \in \mathcal{A}$ since there is no binding with other system criteria to enforce the service-level agreement and avoiding the emptiness of the protected set S . Thereby, a minimum coverage requirement will be considered below, along with a cost-congestion tradeoff, and tail-risk control. Such assessment criteria will be incorporated to the base model through objective functions and additional constraints, as described next.

Assessment Criteria

The proposed framework supports a flexible family of objectives and constraints that capture economic efficiency, congestion robustness, service coverage, and tail-risk control within a single optimization model.

- **Cost and congestion robustness.** Operating capacity is penalized through a linear cost term $c^t \mu := \sum_{r \in \mathcal{R}} c_r \mu_r$, where $c \in \mathbb{R}_+^R$ represents regime-specific capacity costs. To discourage operation close to instability, we also incorporate a logarithmic congestion penalty of the form $-\log(\mu_r - \Lambda_r)$, which increases rapidly as the service slack approaches zero. Introducing auxiliary variables ν_r , this penalty can be modeled via the exponential cone constraints

$$(\mu_r - \Lambda_r, 1, \nu_r) \in \mathcal{K}_{\text{exp}}, \quad \forall r \in \mathcal{R}. \quad (7)$$

These expressions mean $\mu_r - \Lambda_r \geq e^{\nu_r}$, so that $\log(\mu_r - \Lambda_r) \geq \nu_r$ for all regime $r \in \mathcal{R}$. Thus, $-\nu_r$ provides an upper bound on the logarithmic congestion penalty $-\log(\mu_r - \Lambda_r)$. A representative objective function is therefore given by

$$\min \quad c^t \mu - \kappa \sum_{r \in \mathcal{R}} \nu_r, \quad (8)$$

where $\kappa \geq 0$ controls the emphasis placed on congestion robustness relative to capacity cost.

- **Coverage.** To prevent service guarantees from being concentrated on a negligible subset of the demand population, we impose a minimum coverage requirement of the form

$$\sum_{a \in \mathcal{A}} s_a \geq \lceil \beta |\mathcal{A}| \rceil, \quad (9)$$

where $\beta \in (0, 1]$ specifies the minimum fraction of demand points for which probabilistic service-level agreements must be enforced. The parameter β thus provides a direct and interpretable control on the breadth of service commitments. Larger values of β correspond to near-uniform protection across the population, whereas smaller values allow resources to be focused on a core subset of demand elements where guarantees can be delivered most cost-effectively.

The framework readily accommodates extensions of (9) to account for heterogeneity in demand importance or economic value. For example, letting $w_a > 0$ denote a weight associated with element a , a weighted coverage constraint of the form

$$\sum_{a \in \mathcal{A}} w_a s_a \geq \beta \sum_{a \in \mathcal{A}} w_a$$

ensures protection of a prescribed fraction of total weighted demand. Moreover, β itself may be treated as a decision variable, enabling the model to determine the maximum achievable coverage under a fixed budget or congestion limit.

- **Conflict-aware service guarantees.** Meanwhile the coverage constraint (9) ensures that a minimum fraction of demand elements is protected, in practice it may not be operationally credible to enforce strict service-level guarantees for all selected elements simultaneously. In congested service systems, guarantees compete for localized and highly correlated resources, such as nearby servers, dispatch units, or priority capacity, particularly under adverse demand realizations that drive tail-risk measures.

To prevent over-commitment of such resources, we introduce conflict constraints that restrict simultaneous protection of incompatible demand elements. These constraints are modeled via a conflict graph $G = (\mathcal{A}, \mathcal{E})$, where each node $a \in \mathcal{A}$ represents a demand element and an edge $\{a, a'\} \in \mathcal{E}$ indicates that elements a and a' cannot both be assigned strict service guarantees without violating operational feasibility. The conflict constraints take the simple linear form

$$s_a + s_{a'} \leq 1, \quad \forall \{a, a'\} \in \mathcal{E}. \quad (10)$$

The conflict graph can be constructed using empirical information on spatial proximity, temporal overlap, shared service resources, or correlation of response times under congestion.

By explicitly modeling such incompatibilities, constraint (10) ensures that the protected set of demand elements remains operationally credible, preserves the integrity of the service guarantees under tail-risk control, and prevents the model from relying on unrealistic concentration of guarantees in highly congested regions of the system, in line with the congestion interaction effects discussed in [Feldman and Tamir \[2012\]](#).

- **Tail-risk control.** Note that although (9) is selectively enforced on a β fraction of the users, it might also be important to control the performance experienced by the remaining $1 - \beta$ proportion who may face consistently high response times. To prevent unbounded degradation among these users, one may incorporate a complementary robust condition based on the average of the expected time of those customers who could *violate* the SLA constraints $(\mathcal{A} \setminus S)$. To adapt the formulation to this feature, it considers a time threshold value $\Gamma \geq 0$ which will upper bound the expected response times of the users in $\mathcal{A} \setminus S$, and adds the nonlinear constraint

$$\frac{1}{[(1 - \beta)|\mathcal{A}|]} \sum_{a \in \mathcal{A}} (1 - s_a) \left(t_a + \sum_{r \in \mathcal{R}} \frac{\pi_r}{\mu_r - \Lambda_r} \right) \leq \Gamma.$$

Despite its nonlinearity, it can be replaced by $|\mathcal{R}|$ exponential cone constraints, $3|\mathcal{A}||\mathcal{R}| + 1$ linear constraints, and $(|\mathcal{A}| + 1)|\mathcal{R}|$ continuous auxiliary variables, keeping convexity in its continuous relaxation. Nevertheless, this constraint just ensures proper robustness in case all demand in $\mathcal{A} \setminus S$ actually violate the SLA constraints, i.e., $\mathbb{P}(R_a \leq t_a^*) < 1 - \alpha_a, \forall a \in \mathcal{A} \setminus S$. A careful reader will notice this forced-violation requirement would suppose a nonsense for the aim of guaranteeing the quality of the service. Because of that, we will tackle robustness in expected response times via conditional value-at-risk (CVaR), which allows us to split the coverage of the strictly satisfied demand and the tail-risk control. This is performed through the notion of CVaR

$$\text{CVaR}_\gamma(\mathbb{E}[R_a]_{a \in \mathcal{A}}) := \frac{1}{\lfloor (1 - \gamma)|\mathcal{A}| \rfloor} \sum_{i=1}^{\lfloor (1 - \gamma)|\mathcal{A}| \rfloor} \mathbb{E}[R_{(i)}]$$

where $\mathbb{E}[R_{(1)}] \geq \mathbb{E}[R_{(2)}] \geq \dots \geq \mathbb{E}[R_{(|\mathcal{A}|)}]$ is the (non-increasing) sorted list of expected total response times of each of the demands, and $0 < 1 - \gamma \leq 1$ is the proportion of the demand with the worst expected total response times (γ could be β or could be decoupled from the coverage condition). That means $\text{CVaR}_\gamma \circ \mathbb{E}$ is the average of the expected response time of the demands whose expected total response are among the $1 - \gamma$ worst fraction.

Lemma 2. *Let \mathcal{A} be the set of demands, $0 \leq \gamma < 1$ be a proportion, and $\Gamma \geq 0$ be a time threshold. The condition $\text{CVaR}_\gamma(\mathbb{E}[R_a]_{a \in \mathcal{A}}) \leq \Gamma$ can be expressed with the following set of exponential cone constraints*

$$r_a \geq t_a + \sum_{r \in \mathcal{R}} \pi_r \tau_r, \quad \forall a \in \mathcal{A}, \quad (11)$$

$$U_a \geq r_a - \eta, \quad \forall a \in \mathcal{A} \quad (12)$$

$$\eta + \frac{1}{\lfloor (1 - \gamma)|\mathcal{A}| \rfloor} \sum_{a \in \mathcal{A}} U_a \leq \Gamma, \quad (13)$$

$$\nu_r + \ell_r \geq 0, \quad \forall r \in \mathcal{R}, \quad (14)$$

$$(\tau_r, 1, \ell_r) \in \mathcal{K}_{\text{exp}}, \quad \forall r \in \mathcal{R}, \quad (15)$$

where (r, τ, η, ℓ, U) are nonnegative auxiliary variables.

Proof. First, we show constraints (14) and (15) ensure $(\mu_r - \Lambda_r)\tau_r \geq 1$. On the one hand, by (15) we have $\tau_r \geq e^{\ell_r}$ therefore $\log(\tau_r) \geq \ell_r$ and by definition of the auxiliary variable ν_r (7) $\log(\mu_r - \Lambda_r) \geq \nu_r$. It implies using (14) that $\log(\mu_r - \Lambda_r) + \log(\tau_r) \geq 0$, hence $(\mu_r - \Lambda_r)\tau_r \geq 1$ holds.

On the other hand, we have that,

$$r_a \geq t_a + \sum_{r \in \mathcal{R}} \pi_r \tau_r \geq t_a + \sum_{r \in \mathcal{R}} \frac{\pi_r}{\mu_r - \Lambda_r} = \mathbb{E}[R_a], \quad (16)$$

for all $a \in \mathcal{A}$, where the first inequality is (11), the second one is due to $(\mu_r - \Lambda_r)\tau_r \geq 1$, and the last equality comes from Theorem 1.

Finally, constraints (12) and (13) bound the largest $1 - \gamma$ proportion of r_a variables [see, e.g., Ogryczak and Tamir, 2003, for the formulation of the k -sum]. Thus, we

obtain

$$\begin{aligned}
\Gamma &\geq \eta + \frac{1}{\lfloor (1-\gamma)|\mathcal{A}| \rfloor} \sum_{a \in \mathcal{A}} U_a, & [\text{by (13)}] \\
&\geq \eta + \frac{1}{\lfloor (1-\gamma)|\mathcal{A}| \rfloor} \sum_{\substack{a \in \mathcal{A}: \\ r_a \geq \eta}} (r_a - \eta), & [\text{by } U \geq 0, (12)] \\
&= \frac{1}{\lfloor (1-\gamma)|\mathcal{A}| \rfloor} \sum_{i=1}^{\lfloor (1-\gamma)|\mathcal{A}| \rfloor} r_{(i)} \\
&\geq \frac{1}{\lfloor (1-\gamma)|\mathcal{A}| \rfloor} \sum_{i=1}^{\lfloor (1-\gamma)|\mathcal{A}| \rfloor} \mathbb{E}[R_{(i)}], & [\text{by (16)}] \\
&=: \text{CVaR}_\gamma(\mathbb{E}[R_a]_{a \in \mathcal{A}})
\end{aligned}$$

as it was claimed. \square

The parameters $(\kappa, \beta, \gamma, \Gamma)$ jointly control congestion robustness, service coverage, and tail-risk aversion, allowing the designer to explore a broad range of reliability and efficiency trade-offs within a single unified optimization framework.

Mathematical Optimization Model

Summarizing the modeling and design developments introduced above, the flexible service system design problem can be expressed as a mixed-integer exponential cone optimization model that integrates stability (4), selective service-level guarantees (5)-(6), cost-congestion robustness (7)-(8), minimum coverage requirement (9), conflict-aware service (10), and tail-risk control (11)-(15) within a single formulation. The decision variables include regime-dependent service capacities, SLA activation indicators, and auxiliary variables required to represent queueing performance and risk measures exactly through linear and exponential cone constraints. The full resulting model is denoted as **SSD(C/TR)-ECP** and can be explicitly found in Appendix A.

The parameters $((\alpha_a)_{a \in \mathcal{A}}, \kappa, \beta, \gamma, \Gamma)$ provide interpretable levers that shape the resulting system design and allow the decision-maker to explore trade-offs between coverage, reliability, congestion robustness, and tail-risk control. The coverage parameter β controls the minimum fraction of demand points for which service-level agreement is enforced. Larger values of β promote more uniform protection across the demand population, typically requiring higher service capacities and leading to more conservative designs, while smaller values allow the model to concentrate resources on a core subset of demand points for which guarantees can be delivered most cost-effectively.

The SLA tolerance parameters α_a governs the strictness of the probabilistic response-time guarantees. Smaller values of α_a impose tighter reliability requirements by limiting the allowable probability of SLA violation for demand a , which in turn increases the required service slack and capacity investment. Larger values of α_a relax these guarantees, allowing higher violation probabilities and yielding less conservative designs.

Tail-risk considerations are controlled through the parameters γ and Γ . The first one sets the proportion of the out-of-tail population, considering the remaining $1 - \gamma$ proportion as the least-favored users to be cared for (typically, one could link the coverage with the tail control taking $\gamma = \beta$). The second one bounds the conditional value-at-risk of the expected

response times across the demand population. Smaller values of Γ enforce stricter control of extreme delays by limiting the average response time experienced by the worst-performing subset of demand points, whereas larger values permit greater variability in tail performance and prioritize cost efficiency.

The congestion-robustness parameter κ balances operating cost against proximity to instability. Increasing κ penalizes designs that operate with small service slack, encouraging capacity buffers and smoother performance under demand fluctuations, while $\kappa = 0$ yields cost-minimizing solutions that may operate closer to critical utilization levels.

Together with the stability margin ε , which enforces a strict buffer away from instability and improves numerical robustness, these parameters define a flexible design space. By varying $((\alpha_a)_{a \in \mathcal{A}}, \kappa, \beta, \gamma, \Gamma)$, the framework can generate a spectrum of solutions ranging from cost-efficient designs with limited coverage and relaxed reliability requirements to highly robust systems with broad service guarantees and controlled tail performance. This parametric structure supports sensitivity analysis and policy evaluation, enabling decision makers to align operational performance with strategic reliability objectives.

Theorem 2. *If $\mathcal{E} \neq \emptyset$, the mixed-integer exponential cone program **SSD(C/TR)-ECP** is NP-hard, even for a single regime, $|\mathcal{R}| = 1$.*

Proof. Proof. Let us consider the simplified version of the problem where $\mathcal{R} = \{1\}$ with $\pi_1 = 1$. One can set $\varepsilon = -\min_{a \in \mathcal{A}} \frac{\log(\alpha_a)}{t_a^* - t_a} > 0$, then take $\mu_1 = \Lambda_1 + \varepsilon$ and enforce $\zeta_{a1} = e^{-\varepsilon(t_a^* - t_a)}$. It is easy to check this choice is feasible for the problem. Finally, choose $\kappa = c_1 = 0$ and pick $(\tau_1, \ell_1, \nu_1, \eta, r, U)$ so that the remaining constraints are trivially satisfied (e.g., take Γ sufficiently large and $\tau_1 = 0$).

Under these parameter choices, the only nontrivial constraints on s are exactly

$$\sum_{a \in \mathcal{A}} s_a \geq \lceil \beta |\mathcal{A}| \rceil \quad \text{and} \quad s_a + s_{a'} \leq 1, \quad \forall \{a, a'\} \in \mathcal{E},$$

so a feasible solution exists if and only if $G = (\mathcal{A}, \mathcal{E})$ contains an independent set of size at least $\lceil \beta |\mathcal{A}| \rceil$. Hence, the problem reduces to the independent set problem, whose feasibility is well-known to be NP-complete [see, e.g., [Garey and Johnson, 2002](#)]. Thus, the optimization problem is NP-hard. \square

3.1. Solution Approach. The problem described above admits a natural decomposition structure in which the binary variables s determine the subset of demand elements for which service-level guarantees are enforced, while all remaining variables enter through a continuous convex optimization problem. Specifically, the problem can be equivalently written as

$$\begin{aligned} & \min \theta \\ \text{s.t. } & \sum_{a \in \mathcal{A}} s_a \geq \lceil \beta |\mathcal{A}| \rceil, \\ & s_a + s_{a'} \leq 1, \quad \forall \{a, a'\} \in \mathcal{E}; \\ & \theta \geq \Theta(s), \\ & s_a \in \{0, 1\}, \quad \forall a \in \mathcal{A}, \end{aligned}$$

where $\Theta(s)$ denotes the optimal value of a (continuous) exponential cone program obtained by fixing s (see [Appendix B](#)).

For any fixed s , the subproblem defining $\Theta(s)$ is a convex optimization problem involving linear constraints and exponential cones. Under standard regularity conditions ensuring feasibility and strong duality, the value function $\Theta(\cdot)$ is convex over the domain $[0, 1]^{\mathcal{A}}$. This

structure enables the use of Benders decomposition, in which the value function $\Theta(\cdot)$ is approximated from below by a sequence of supporting hyperplanes derived from dual information of the subproblem.

The resulting algorithm alternates between a mixed-integer linear master problem in the s -variables and a continuous exponential cone subproblem. At each iteration, the master problem proposes a candidate protection pattern, which is evaluated by solving the subproblem. If the subproblem is feasible, dual multipliers yield a valid Benders optimality cut that is added to the master. If the subproblem is infeasible, a feasibility cut excluding the current solution is generated. The procedure terminates when the optimality gap falls below a prescribed tolerance.

The detailed formulation of the subproblem and the derivation of Benders cuts are provided in Appendix B.

Observe that the master problem has a finite number of feasible binary vectors $s \in \{0, 1\}^{\mathcal{A}}$. In the described decomposition procedure, each iteration adds a cut that excludes the current solution from being optimal unless it is globally optimal. Hence, the procedure cannot revisit the same solution indefinitely and must terminate after finitely many iterations.

3.2. A Polynomial Time Procedure for the Conflict-Free Case. As shown in Theorem 2, problem **SSD(C/TR)-ECP** is NP-hard whenever the conflict graph satisfies $\mathcal{E} \neq \emptyset$. In this section, we explore a structurally important special case in which no conflict constraints are present, that is, $\mathcal{E} = \emptyset$. Although simpler, this setting remains relevant in practice and provides valuable insight into the structure of optimal service guarantee policies.

In many service systems, including emergency medical services, explicit conflicts between demand elements arise primarily due to localized congestion effects. When demand is sufficiently dispersed in time or space, or when the planning horizon is aggregated at a high level, it is reasonable to ignore such pairwise incompatibilities and focus instead on system wide capacity and tail-risk tradeoffs. The conflict-free formulation thus constitutes a useful benchmark and enables analytical characterization of optimal protection strategies. So, throughout this section, we assume $\mathcal{E} = \emptyset$.

We begin by establishing a monotonicity property of the value function $\Theta(\cdot)$.

Proposition 1. *Let $s, s' \in \{0, 1\}^{\mathcal{A}}$ be feasible vectors such that $s \leq s'$ componentwise. Then $\Theta(s) \leq \Theta(s')$.*

Proof. Proof. Assuming that $\mathcal{E} = \emptyset$, the only constraints in the subproblem defining $\Theta(\cdot)$ that depend on s are the coverage constraint

$$\sum_{a \in \mathcal{A}} s_a \geq \lceil \beta |\mathcal{A}| \rceil,$$

and the service-level agreement constraints

$$\sum_{r \in \mathcal{R}} \pi_r e^{-(\mu_r - \Lambda_r) \Delta_a} \leq 1 + (\alpha_a - 1) s_a, \quad \forall a \in \mathcal{A},$$

where $\Delta_a := t_a^* - t_a \geq 0$. Since $\alpha_a < 1$, replacing s by s' tightens these constraints componentwise. Therefore, the feasible region of the subproblem under s' is contained in that under s , and the optimal value cannot decrease. \square

An immediate consequence of this monotonicity is that the coverage constraint can be enforced at equality.

Corollary 2. *There exists an optimal solution satisfying*

$$\sum_{a \in \mathcal{A}} s_a = \lceil \beta |\mathcal{A}| \rceil.$$

Proof. Proof. This is a direct consequence of Proposition 1. \square

In what follows, we additionally assume that $\alpha_a = \alpha$ for all $a \in \mathcal{A}$. That means all demand elements are subject to a common service-level confidence.

This assumption is standard in many practical service systems, where service-level agreement is defined by uniform policy targets rather than individualized confidence requirements. In particular, in emergency service systems and public-sector operations, response-time guarantees are typically specified by system-wide confidence levels reflecting regulatory standards, contractual obligations, or equity considerations. Under this uniform-confidence setting, the conflict-free formulation admits a polynomial-time solution and allows for a clear structural characterization of optimal protection policies.

Theorem 3. *When $\mathcal{E} = \emptyset$ and $\alpha_a = \alpha$ for all $a \in \mathcal{A}$, problem **SSD(C/TR)-ECP** is solvable in polynomial time.*

Proof. Proof. Let $\Delta_a := t_a^* - t_a$ for all $a \in \mathcal{A}$, and let σ be a permutation of \mathcal{A} such that

$$\Delta_{\sigma(1)} \geq \Delta_{\sigma(2)} \geq \cdots \geq \Delta_{\sigma(|\mathcal{A}|)}.$$

The permutation σ can be computed in $\mathcal{O}(|\mathcal{A}| \log |\mathcal{A}|)$ time.

For any feasible service rate vector μ with $\mu_r > \Lambda_r$ for all $r \in \mathcal{R}$, the function

$$f(\Delta) := \sum_{r \in \mathcal{R}} \pi_r e^{-(\mu_r - \Lambda_r)\Delta}$$

is non-increasing in Δ . Hence, if the service-level agreement constraint is satisfied for some index a , it is also satisfied for any index a' with $\Delta_{a'} \geq \Delta_a$.

It follows that, among all selections of $\lceil \beta |\mathcal{A}| \rceil$ protected elements, the least restrictive choice is obtained by selecting the indices with the largest values of Δ_a . Therefore, an optimal solution is obtained by fixing

$$s_a^* = \begin{cases} 1, & \text{if } \sigma(a) \leq \lceil \beta |\mathcal{A}| \rceil, \\ 0, & \text{otherwise,} \end{cases}$$

and solving the resulting continuous exponential cone program with $s = s^*$. Since this subproblem is convex, it can be solved in polynomial time by interior point methods. \square

Note that the ordering argument above relies critically on the assumption of a uniform confidence level. When the parameters α_a are heterogeneous, the restrictiveness of a service-level agreement depends jointly on the temporal slack Δ_a and the tolerance parameter α_a . While larger values of Δ_a make a constraint easier to satisfy, smaller values of α_a impose stricter probabilistic guarantees. As a result, neither parameter alone induces a total ordering, and only a partial order based on simultaneous dominance in both Δ_a and α_a can be established. Consequently, in the heterogeneous confidence case there is no universal scalar sorting rule that determines the optimal protected set, and the polynomial-time selection result no longer applies. However, if there exists a subset of $\lceil \beta |\mathcal{A}| \rceil$ demand elements whose pairs (Δ_a, α_a) dominate those of all remaining elements componentwise, then the same polynomial-time procedure applies by selecting this dominating subset, since their associated service-level agreement constraints are uniformly less restrictive.

Algorithm 1 Polynomial time solution for the conflict-free case and uniform confidence levels.

Input: Set \mathcal{A} , integer $k = \lceil \beta |\mathcal{A}| \rceil$, slacks $\Delta_a = t_a^* - t_a \geq 0$ for all $a \in \mathcal{A}$, and the exponential cone subproblem defining $\Theta(s)$.

1: Compute $\Delta_a = t_a^* - t_a$ for all $a \in \mathcal{A}$.

2: Sort \mathcal{A} in non-increasing order of Δ_a and let σ be the resulting permutation.

3: Define $s^* \in \{0, 1\}^{\mathcal{A}}$ by

$$s_{\sigma(i)}^* = \begin{cases} 1, & i = 1, \dots, k, \\ 0, & i = k + 1, \dots, |\mathcal{A}|. \end{cases}$$

4: Solve the exponential cone program defining $\Theta(s^*)$ to obtain μ^* .

5: **return** (s^*, μ^*) .

Output: An optimal solution (s^*, μ^*) to [SSD\(C/TR\)-ECP](#).

Summarizing, note that the result above highlights a sharp contrast between the general conflict-aware formulation and the conflict-free case. When no incompatibilities are present, the optimal protection policy admits a simple threshold structure based on the temporal slack Δ_a . Introducing conflict constraints destroys this ordering property and leads to combinatorial selection effects that render the problem NP-hard, as established earlier.

4. NUMERICAL EXPERIMENTS: NYC EMS CASE STUDY

We assess the proposed exponential conic optimization framework using real incident-level data from the New York City Emergency Medical Services (EMS) system ([data.cityofnewyork.us](#)). The goal of the experiments is twofold. First, we evaluate the computational performance of the proposed compact formulation against the Benders decomposition algorithm developed in this paper. Second, we analyze the managerial implications of the optimized service rates under different congestion and tail-risk profiles.

The dataset is obtained from the NYC Open Data EMS Incident Dispatch repository from 2025 and contains individual emergency calls with detailed information about each incident. We construct our input dataset and parameters for our approach based on the following elements.

- **Boroughs.** We partition the whole dataset based on the borough where the incident occurred. We focus our analysis on the four most populated NYC boroughs: Manhattan, Bronx, Brooklyn, and Queens.
- **Regimes.** We consider that the regimes represent different initial call types from the EMS incidents, namely **CARDBR** (difficulty breathing with chest pain), **INJURY** (non-critical), **SICK**, and **UNC** (unconscious patient).
- **Time window scenarios.** We restrict the datasets to different time window scenarios within 2025 to generate datasets of different sizes and characteristics. In particular, we focus on: two scenarios based on incidents that occurred in night/peak hours within a single day; three scenarios based on single but whole days; and three scenarios for three days in a row, a week, and a year, respectively. The precise starting and ending instants (date/time) of each time window are detailed in Table 1 (right) and the sizes of each of the constructed datasets is shown in Table 2 (column $|\mathcal{A}|$).
- **Parameter profiles.** We consider several service-level profiles reflecting different trade-offs between coverage, congestion, and tail-risk aversion. Each profile is characterized by: (i) a target coverage level β , which also determines the proportion of

out-of-tail demand used in the conditional value-at-risk (CVaR), i.e., we set $\gamma = \beta$; (ii) a risk-aversion parameter ψ controlling the CVaR threshold $\Gamma(\psi)$; (iii) a slack parameter α regulating the tolerance on response-time compliance; (iv) a regularization parameter κ penalizing excessive service capacity; (v) a scaling parameter φ defining the upper bound, $t_a^*(\varphi)$ in the SLA constraints as a percentage of the actual completion time t_a^c , namely, $t_a^* = \varphi t_a^c$. The profiles range from strict high-coverage configurations to more flexible designs that allow greater congestion in exchange for reduced capacity requirements. The detailed parameter combinations are reported in Table 1 (left).

The six profiles represent distinct operational philosophies, namely:

- **BAL (balanced).** A high coverage level ($\beta = 0.95$) combined with moderate slack and neutral SLA scaling ($\varphi = 1$) yields a benchmark configuration that balances reliability and capacity investment without emphasizing extreme tail protection.
- **COV (coverage-oriented).** A lower coverage target ($\beta = 0.80$) but a slightly relaxed SLA bound ($\varphi = 1.03$) shifts the focus toward average compliance rather than strict worst-case performance.
- **HARD (stringent compliance).** A very small tolerance ($\alpha = 0.02$) and tighter SLA scaling ($\varphi = 0.95$) impose strict response-time requirements and typically lead to higher required service capacity.
- **REL (reliability-focused).** Lower coverage ($\beta = 0.70$) but strong tail aversion ($\psi = 1.25$) emphasizes protection against extreme delays rather than universal compliance.
- **TAIL+ (tail protection under tight compliance).** Very small tolerance ($\alpha = 0.01$) combined with neutral SLA scaling ($\varphi = 1$) enforces tight compliance while focusing on delay dispersion control.
- **TIGHT+ (aggressive SLA tightening).** A substantially reduced SLA bound ($\varphi = 0.88$) makes response-time targets significantly stricter than historical completion times and typically requires substantial capacity upgrades.

Overall, the profiles allow decision-makers to explicitly quantify the trade-off between investment in capacity (through κ and the induced service rates) and reliability guarantees (through β , ψ , α , and φ). Stricter SLA scaling and smaller slack parameters increase robustness and punctuality but at the expense of higher operational costs, while more relaxed configurations reduce capacity needs at the cost of greater congestion risk.

- **Conflict graphs.** From each filtered dataset, we build an undirected conflict graph whose nodes correspond to individual EMS incidents. Two incidents are connected by an edge if they occur sufficiently close in time and space, capturing short-term competition for shared resources. Incidents are grouped by dispatch area and ordered by time. Within each group, we connect any two incidents whose occurrence times differ by at most one minute. The resulting graph captures short temporal bursts of demand within the same operational area.

For each borough, scenario, and profile, we solve the service system design problem using two approaches. The first is the compact mixed-integer exponential cone formulation [SSD\(C/TR\)-ECP](#) solved directly with the mixed-integer conic optimizer Mosek. The second is the Benders decomposition scheme, described in Section 3.1 and detailed in Appendix B, in which the master problem determines the set of protected users (under coverage and conflict constraints), while subproblem yields service rates, evaluates the tail-risk and service-level

TABLE 1. Service-level profiles (left) and observation windows (right) used in the experiments.

Profile	β	α	ψ	φ	κ	Scenario	Start	End
BAL	0.95	0.05	1.10	1.00	0.10	night	2025-03-03 20:00	2025-03-04 08:00
COV	0.80	0.07	1.15	1.03	0.10	peak	2025-03-03 08:00	2025-03-03 20:00
HARD	0.90	0.02	1.05	0.95	0.10	D1	2025-03-01 00:00	2025-03-02 00:00
REL	0.70	0.10	1.25	1.08	0.10	D2	2025-03-02 00:00	2025-03-03 00:00
TAIL+	0.75	0.01	1.00	1.00	0.10	D3	2025-03-03 00:00	2025-03-04 00:00
TIGHT+	0.80	0.05	1.08	0.88	0.10	3days	2025-03-01 00:00	2025-03-04 00:00
						week	2025-03-01 00:00	2025-03-08 00:00
						year	2025-01-01 00:00	2026-01-01 00:00

TABLE 2. Summary of sizes, mixture probabilities, and conflict edges for each borough and scenario in our experiments.

Borough	Scenario	$ \mathcal{A} $	$ \mathcal{E} $	π	Borough	Scenario	$ \mathcal{A} $	$ \mathcal{E} $	π
Bronx	night	110	3	(0.3182, 0.2455, 0.3273, 0.1091)	Manhattan	night	101	2	(0.3168, 0.2574, 0.2772, 0.1485)
	peak	178	10	(0.3539, 0.2303, 0.2079, 0.2079)		peak	165	8	(0.2061, 0.3697, 0.2424, 0.1818)
	D1	243	6	(0.2675, 0.2387, 0.3004, 0.1934)		D1	263	10	(0.1711, 0.3156, 0.2928, 0.2205)
	D2	236	6	(0.3390, 0.3051, 0.2331, 0.1229)		D2	233	2	(0.2275, 0.3219, 0.2833, 0.1674)
	D3	287	15	(0.3693, 0.2125, 0.2369, 0.1812)		D3	259	9	(0.2394, 0.3359, 0.2548, 0.1699)
	3days	576	19	(0.3455, 0.2535, 0.2413, 0.1597)		3days	526	11	(0.2262, 0.3213, 0.2757, 0.1768)
	week	1781	73	(0.3088, 0.2718, 0.2673, 0.1522)		week	1887	55	(0.2194, 0.3153, 0.2719, 0.1934)
Brooklyn	night	104	5	(0.2596, 0.2981, 0.3558, 0.0865)	Queens	night	86	0	(0.1977, 0.3372, 0.2674, 0.1977)
	peak	195	5	(0.2821, 0.2974, 0.2410, 0.1795)		peak	129	2	(0.2403, 0.2791, 0.3101, 0.1705)
	D1	321	9	(0.2087, 0.3115, 0.3084, 0.1713)		D1	209	6	(0.2057, 0.3254, 0.3014, 0.1675)
	D2	299	11	(0.2408, 0.2575, 0.2977, 0.2040)		D2	226	5	(0.1991, 0.3717, 0.2699, 0.1593)
	D3	316	8	(0.2911, 0.2943, 0.2690, 0.1456)		D3	228	3	(0.2325, 0.3246, 0.2719, 0.1711)
	3days	684	24	(0.2617, 0.2822, 0.2880, 0.1681)		3days	495	10	(0.2141, 0.3515, 0.2727, 0.1616)
	week	2209	73	(0.2399, 0.2947, 0.2988, 0.1666)		week	1613	42	(0.2381, 0.3292, 0.2858, 0.1469)

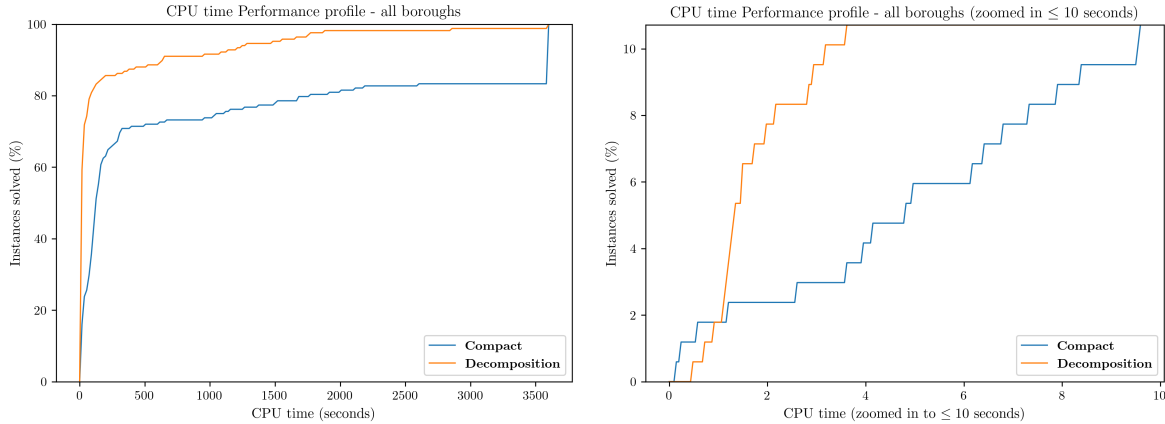
Note: the summary for scenario YEAR is detailed in Table 3.

constraints, and generate cutting planes. Both approaches are implemented in Mosek Fusion Python API using the same solver settings. All instances were solved with Gurobi 12 on macOS running on a Mac Studio equipped with an Apple M1 Max chip (10-core CPU: 8 performance and 2 efficiency cores) and 64 GB of unified memory.

The computational study compares the two approaches in terms of total running time, number of instances solved to optimality within the time limit, and objective value consistency. This allows us to assess the scalability and numerical robustness of the proposed decomposition relative to the compact model.

In the second part of the analysis, we examine the structure of the optimized solutions. We study how total response times (and its CVaR), congestion level, and cost vary across boroughs and profiles. These results provide managerial insights into how congestion control and tail-risk constraints shape optimal EMS service design decisions in large urban systems.

Computational Performance. We begin by assessing the overall computational performance of the two solution approaches, namely the compact mixed-integer exponential cone formulation (**compact**) and the decomposition strategy described in Section 3.1 and Appendix B (**decomposition**).



Performance profile of CPU time for all instances (left) and zoomed view for those solved within 10 seconds (right).

Figure ?? presents the corresponding performance profiles, reporting the percentage of instances solved within a given CPU time. The left panel shows the full time horizon, while the right one zooms into instances solved within 10 seconds (approximately 10% of the sample), highlighting early-time behavior.

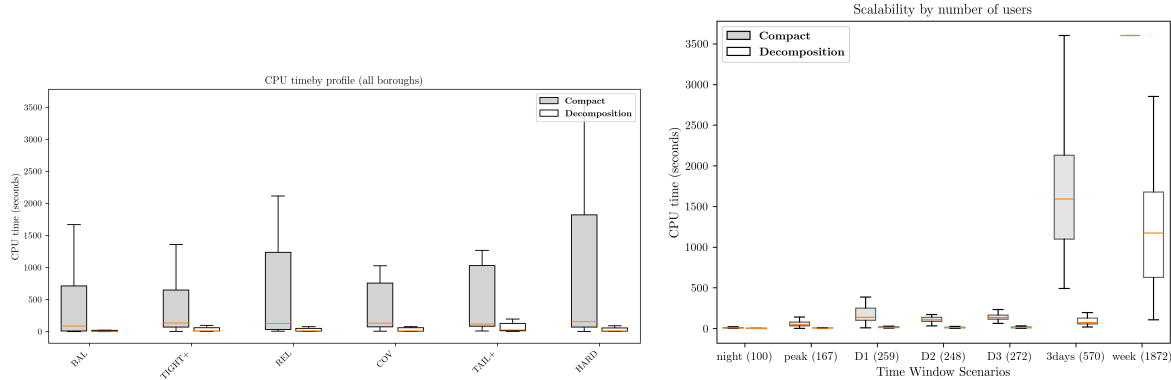
The **decomposition** approach exhibits a markedly steeper growth from the very first seconds, solving a substantial fraction of instances almost immediately and reaching near-complete coverage significantly earlier than the **compact** formulation. In contrast, the compact model displays slower progress and a pronounced computational tail, with a non-negligible subset of instances requiring substantially longer running times.

When all instances are considered jointly, the dominance of the decomposition strategy is evident across the entire time spectrum. Not only does it solve easy instances rapidly, but it also shows significantly greater stability when confronted with large-scale or structurally challenging cases. The compact formulation, by comparison, is considerably more sensitive to difficult parameter configurations, leading to delayed convergence and heavier tail behavior. Performance profiles disaggregated by borough are reported in Appendix C, where the same qualitative pattern consistently holds.

The global profile clearly illustrates the principal computational advantage of the decomposition approach: while both methods handle the easiest instances efficiently, the decomposition remains robust as instance size and difficulty increase. This feature is particularly valuable in exploratory, sensitivity, or scenario-based analyses, where a large number of related instances must be solved repeatedly and predictable computational effort is essential.

Consistently with the performance profiles, 25% of the instances were not solved to proven optimality within the one-hour time limit when using the **compact** formulation. Among the unsolved instances, the average residual MIP gap equals 58.60% in Bronx, 58.70% in Brooklyn, 68.82% in Manhattan, and 51.70% in Queens. These gaps further confirm that the compact formulation struggles on a substantial subset of challenging instances, whereas the decomposition approach achieves markedly stronger overall time-to-solution performance with all instances optimally solved.

In order to assess the computational impact of the different profiles (and, indirectly, of the parameter configurations they induce), Figure ?? reports boxplots of CPU times (in seconds)



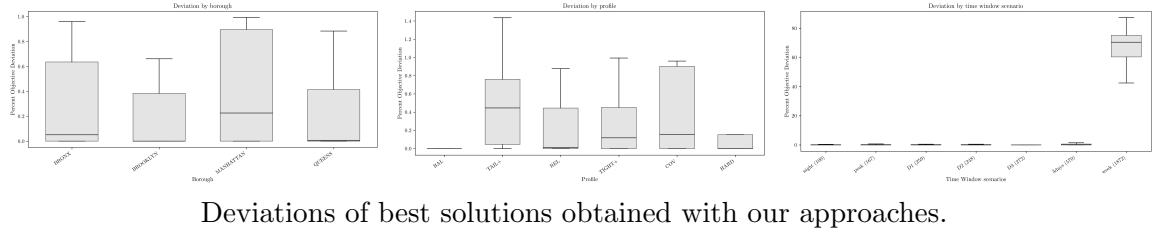
Boxplots of CPU time by profile (left) and time window scenario (right). The distribution of CPU times is shown for the **compact** and **decomposition** approaches.

for each profile (left) and time window scenario (right), comparing the **compact** and **decomposition** approaches removing outlier instances from both approaches. In Appendix C, the reader can found the analogous boxplots disaggregated by borough.

Across all profiles, the **decomposition** approach yields substantially smaller CPU times and a much tighter dispersion, with medians close to the origin and comparatively short upper whiskers. In contrast, the **compact** formulation exhibits large variability and a pronounced right tail in every profile, with many instances approaching the one-hour limit. The gap between both approaches becomes particularly visible for the most demanding profiles TAIL+, COV, and HARD, where the compact model shows heavy-tailed behavior and frequent time-limit hits, while the **decomposition** remains consistently fast and stable. Overall, these boxplots reinforce the conclusions from the performance profiles: the **decomposition** strategy is markedly less sensitive to adverse parameter combinations and provides substantially more predictable computational effort across scenarios. For the different time window scenarios, that also represent different number of users/incidents, a clear monotonic trend is observed for both approaches: CPU times increase as the average number of users grows, with the most pronounced effects occurring in the 3DAYS and WEEK scenarios (triplicating in average the number of users/incidences). However, as we have already observed the growth rate differs substantially between formulations. The **compact** model exhibits a sharp increase in both median solution time and dispersion as the number of users rises, together with heavy-tailed behavior and frequent time-limit hits in the largest scenarios. In contrast, the **decomposition** approach scales significantly more gracefully: although computation times increase for larger windows, the median and interquartile ranges remain markedly smaller, and the variability is substantially reduced.

The difference becomes particularly striking in the WEEK scenario, where the **compact** formulation frequently approaches consistently the one-hour limit, whereas the **decomposition** method maintains substantially lower median times and improved stability. Overall, these results confirm that the **decomposition** strategy not only accelerates solution times in small and medium instances, but also provides superior scalability and robustness as the problem dimension increases.

Finally, we analyze the managerial implications of solving the proposed problem efficiently. In particular, we compare the quality of the objective values obtained by the two approaches on the same instances. Although the **compact** formulation is computationally more demanding than the **decomposition** approach to certify optimality, one might expect that both methods



Deviations of best solutions obtained with our approaches.

eventually identify solutions of comparable quality within the time limit. However, this is generally not the case.

To quantify these differences, we report the relative percent deviation of the best solution obtained with the **compact** formulation with respect to the optimal solution provided by the **decomposition** approach. Specifically, we define

$$\text{dev} = 100 \frac{\text{BestObj}_{\text{compact}} - \text{OptObj}_{\text{decomposition}}}{\text{BestObj}_{\text{compact}}} \%$$

Since the **decomposition** approach solves the instances to optimality within the time limit, this deviation is always nonnegative and measures the loss in solution quality incurred by relying on the **compact** formulation under time constraints.

Figure ?? presents boxplots of these deviations disaggregated by borough (left), profile (center), and time window scenario (right).

The results reveal substantial variability in the quality loss associated with the **compact** formulation. By profile, the largest deviations occur under the more demanding configurations (notably TAIL+ and COV), where both the median and dispersion are markedly higher. In contrast, the BAL profile exhibits negligible deviations, indicating that easier parameter regimes allow both approaches to achieve similar solutions within the time limit.

The time-window analysis highlights an even more pronounced effect of problem scale. While short windows (e.g., NIGHT, PEAK, and daily scenarios) display near-zero deviations, the WEEK scenario shows dramatically larger percent deviations, with consistently high medians and limited overlap with smaller windows. This confirms that as the number of users increases, the **compact** formulation struggles not only in computational time but also in solution quality.

Finally, the borough-level results indicate that Manhattan exhibits systematically larger deviations and greater dispersion, suggesting that its instances are structurally more challenging from a computational standpoint. Overall, these findings demonstrate that the **decomposition** approach delivers not only superior computational efficiency but also substantially improved solution quality in large-scale and demanding scenarios. From a managerial perspective, this distinction is critical: achieving proven optimality is essential, since prematurely terminating the solution process at the time limit may result in significant losses in objective value, particularly in the most complex and large-scale input data.

Case Study: Managerial Insights from a Borough Level Urban Service System. After completing the computational performance analysis, we now turn to the managerial implications of the proposed framework. To this end, we consider a large-scale case study based on the complete EMS NYC dataset for the year 2025, extracted and processed analogously to the experimental setting described above. In contrast to the controlled benchmarking instances used for performance evaluation, this dataset reflects the full operational scale of the system over an entire year, thereby providing a realistic and practically meaningful environment for policy analysis.

TABLE 3. Estimated mixture weights π by service regime and user population sizes by borough for the full-year 2025 dataset.

Borough	π by service regime				
	CARDBR	INJURY	SICK	UNC	Incidents
Manhattan	0.1967	0.2893	0.2473	0.2667	66,780
Bronx	0.2897	0.2846	0.2536	0.1721	62,818
Brooklyn	0.2309	0.3013	0.2744	0.1934	79,975
Queens	0.2287	0.3229	0.2711	0.1773	55,681

To facilitate interpretation and isolate the economic trade-offs induced by the service design decisions, we omit the conflict constraints in this analysis. In this setting, the resulting problem becomes polynomially solvable via Algorithm 1, allowing us to focus exclusively on structural and managerial insights rather than computational limitations. The problems for the different boroughs were solved in 45 seconds in average (max: 80 seconds, min: 28 seconds). The sizes of the borough-level instances and the estimated mixture weights π , capturing heterogeneous service-time regimes, are reported in Table 3.

The goal of this section is to quantify and interpret the trade-offs embedded in the proposed service system design. In particular, we address four central managerial questions:

- **The price of efficiency.** What is the gain in total response time achieved by the proposed design relative to baseline configurations?
- **The price of congestion control.** How does the design affect system load and operational stability?
- **The price of fairness.** To what extent does the model protect the least-favored users?
- **The price of robustness.** What is the cost of incorporating robustness in the service system design?

The terminology follows the seminal notion of the *price of robustness* introduced by [Bertsimas and Sim \[2004\]](#), adapted here to the multi-criteria service system context. By analyzing these four dimensions jointly, we provide a comprehensive assessment of the operational, economic, and societal implications of the proposed optimization framework under realistic large-scale conditions.

To compare the proposed service system design with the one effectively implemented in practice, we first estimate the service rates of the queueing system from historical data. Specifically, for each borough and call type (service regime), we compute empirical service-time estimates based on observed incident durations. Let S denote the sojourn time in minutes, obtained as the difference between the assignment time and the incident close time for valid observations (i.e., strictly positive and finite durations). For each call type r , we compute the sample mean of the sojourn time $\hat{s}_r = \frac{1}{n_r} \sum_{i=1}^{n_r} S_{ri}$, where n_r is the number of valid observations for regime r .

The estimated service rate is constructed as $\hat{\mu}_r = \frac{1}{\hat{s}_r} + \Lambda_r$, where Λ_r denotes the empirical arrival rate of the system under regime r . This adjustment accounts for the effective workload in the observed system configuration and ensures consistency with the steady-state balance condition of the queue. These borough- and regime-specific service rates provide a data-driven proxy of the performance of the current status quo system, which serves as the benchmark

TABLE 4. Estimated arrival rates Λ_r , service rates $\hat{\mu}_r$, and average service times $1/\hat{\mu}_r$ by borough and regime.

Borough	Arrival rates (Λ)			Service rate ($\hat{\mu}$)			Avg. service time in minutes ($1/\hat{\mu}$)					
	CARDR	INJURY	SICK	UNC	CARDR	INJURY	SICK	UNC	CARDR	INJURY	SICK	UNC
Manhattan	0.0375	0.0552	0.0472	0.0509	0.0505	0.0712	0.0613	0.0705	19.82	14.05	16.30	14.18
Bronx	0.0520	0.0511	0.0455	0.0309	0.0643	0.0669	0.0591	0.0474	15.55	14.96	16.91	21.09
Brooklyn	0.0528	0.0689	0.0627	0.0442	0.0656	0.0843	0.0762	0.0612	15.24	11.86	13.13	16.34
Queens	0.0364	0.0514	0.0431	0.0282	0.0495	0.0669	0.0570	0.0446	20.18	14.95	17.55	22.43

against which the proposed optimized design is assessed. The resulting estimates, based on the full-year 2025 dataset, are reported in Table 4.

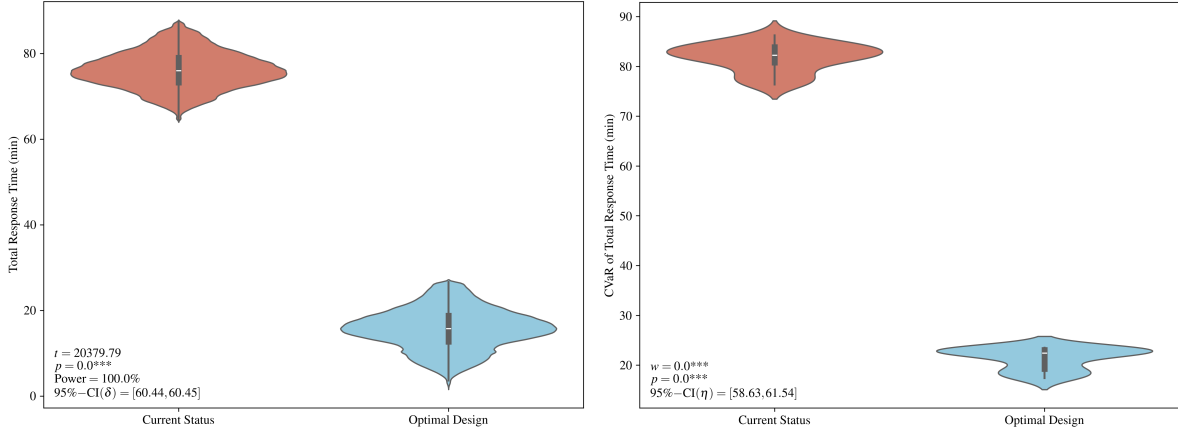
The estimates reveal substantial heterogeneity across boroughs and regimes, both in arrival and service rates. Brooklyn exhibits the highest service rates (particularly under regime 2), whereas Queens and Manhattan display comparatively lower service rates in regimes 1 and 4, which translate into longer average service times. At the same time, arrival rates vary significantly across boroughs, with Brooklyn and Manhattan experiencing consistently higher demand intensities in several regimes.

The joint variation of Λ_r and $\hat{\mu}_r$ implies heterogeneous utilization levels and congestion exposure across the system. In particular, regimes combining high arrival rates with relatively modest service rates are structurally more vulnerable to congestion. These differences highlight the operational imbalance across boroughs and reinforce the importance of borough-specific and regime-aware service system design decisions.

- **The price of efficiency (gains in total response time).** The *price of efficiency* quantifies the reduction in total response time obtained by optimally redesigning the service system relative to the current data-driven configuration. Since response time directly impacts service quality, reliability, and, particularly in emergency settings, safety outcomes, improving this metric is of primary managerial relevance.

Figure ?? presents the global comparison. The left panel shows the full distribution of total response times, and the right panel reports the corresponding conditional value-at-risk (CVaR). The optimized design produces a dramatic and systematic leftward shift of the entire distribution. Median response times decrease by approximately one hour, dispersion is slightly reduced, and extreme delays are significantly mitigated. Statistical tests confirm overwhelming significance. The plots additionally report the results of a parametric paired *t*-test for equality of total response time means (left bottom corner), including the test statistic (*t*), the corresponding *p*-value, the achieved statistical power, and a 95% confidence interval for the effect size (δ), interpreted as the true difference in means. Analogously, in the right plot, we report a summary of the nonparametric paired Wilcoxon test for the homogeneity of CVaR of the total response time groups, including the test statistic (*w*), the *p*-value, and a 95% confidence interval for the true median of the differences (η). For the total response time, values of $p = 0.0^{***}$ and power = 100%, with an estimated mean reduction of roughly 60 minutes and an exceptionally tight confidence interval point out and quantify the price of efficiency. Hence, the improvement is not only statistically significant but also operationally large.

The spatial robustness of these gains is illustrated in Figure ?? (in Appendix D), which disaggregates total response times by borough. In every borough the optimal design uniformly reduces median response times from approximately 70–80 minutes to roughly 15–20 minutes. The reductions are statistically significant in all cases



Global comparison of total response time (left) and its CVaR (right), in minutes, between the current system and the optimal design.

($p = 0.0^{***}$) with extremely large test statistics and narrow confidence intervals for the effect size, confirming that the improvements are consistent across heterogeneous demand environments. Importantly, the effect is uniform in direction: no borough experiences a deterioration, and congestion is not shifted geographically. Instead, the optimized configuration improves efficiency system-wide.

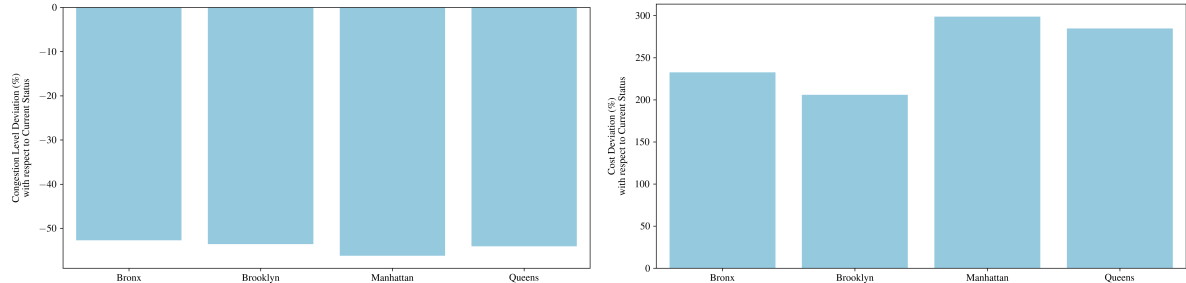
A similar pattern emerges when results are examined by operational profile (see Appendix D). Under the current configuration, median response times remain high across profiles. Under the optimized design, medians fall consistently to the range of 10–20 minutes, with controlled variability. The largest relative gains occur in stringent and tail-focused profiles (HARD, TAIL+, TIGHT+), where the current system incurs substantial efficiency penalties. Even in robustness-oriented profiles (REL, COV), the optimized design achieves clear reductions in both central tendency and dispersion.

Overall, the price of efficiency is uniformly favorable. The optimized design dominates the current configuration globally, spatially, and across design regimes, delivering large, consistent, and statistically robust reductions in total response time. From a managerial perspective, this translates into a faster, more stable, and more reliable service system with significantly lower exposure to extreme delays.

- **The price of congestion control (impact on system load and stability).** Congestion is a primary source of instability and extreme delays in urban service systems. The *price of congestion control* captures the trade-off between reducing system load and the potential cost or efficiency adjustments required to achieve stability.

Under the historically estimated configuration, the system operates persistently close to saturation, leaving little buffer to absorb demand fluctuations. In contrast, the optimal design shifts the distribution of congestion levels downward, introducing structural slack and reducing the likelihood of near-instability regimes. This represents a transition from a brittle operating point to a more resilient and stable configuration.

Figure ?? reports congestion and cost deviations by borough. In the left panel, congestion level reductions are observed uniformly across all boroughs, indicating that improvements are systemic rather than spatially reallocated. The reductions are statistically significant and accompanied by controlled variability, confirming that stability gains are achieved without transferring load between regions. The right panel



Congestion level (left) and cost deviations (right), in %, relative to the current system by borough. Negative values indicate reduced congestion under the optimal design.

shows the associated cost deviations, quantifying the operational adjustment required to secure these congestion reductions.

A similar pattern emerges across operational profiles (see Appendix D). Profiles imposing stringent guarantees or tail protection exhibit the highest congestion under the current system, reflecting the inefficiency of enforcing strict targets without coordinated optimization. Under the optimal design, congestion levels decrease markedly across all profiles, often moving the system away from the saturation boundary. Even balanced profiles experience systematic improvements.

Overall, the cost of congestion control is favorable. The optimized design achieves substantial and statistically significant reductions in system-wide congestion, with reductions exceeding 50% in every borough and ranging from 40% to nearly 80% across the profiles. It enhances system stability without inducing spatial imbalances. These results demonstrate that congestion control can be embedded directly into system design, yielding a structurally more robust and resilient operation than the current configuration.

- **The price of fairness (protection of least-favored users).** Fairness in service systems concerns the protection of users most exposed to extreme delays. The *price of fairness* measures the performance trade-offs required to reduce tail risk, typically assessed through risk-sensitive metrics such as the conditional value-at-risk (CVaR). In this context, fairness does not imply equalizing averages, but limiting exposure to severe service outcomes.

Figure ?? reports borough-level changes in CVaR relative to the current system. Negative values indicate reductions in extreme delays under the optimal design. Substantial and systematic CVaR reductions are observed across all boroughs, with particularly pronounced improvements in high-demand regions such as Brooklyn, Manhattan, and Queens. These results indicate that tail-risk mitigation is structural and not confined to isolated scenarios.

Figure ?? provides the same analysis by operational profile. Under the current configuration, profiles imposing strict guarantees (HARD) exhibit substantial tail exposure, highlighting the inefficiency of enforcing fairness objectives without coordinated optimization. The optimal design markedly reduces CVaR across nearly all profiles, including tail-focused configurations (TAIL+), without transferring risk to other regimes.

The optimized design delivers large and consistent reductions in tail risk across both spatial and operational dimensions. To formally assess the differences in CVaR values reported in Figure ?? (right), we apply the Wilcoxon signed-rank test. The test

yields a p -value below conventional significance levels ($p < 0.001$) and a test statistic of $w = 0$, indicating a systematic reduction in tail risk under the optimized design. The estimated median reduction is approximately one hour. These results support that the proposed design not only cuts the time for the average user but also narrows the gap experienced by the least-favored users, preserving homogeneity and yielding a service system that meets efficiency at the time that promotes robustness and fairness. These findings demonstrate that such objectives can be embedded directly into system design through explicit risk-sensitive optimization, yielding measurable protection for least-favored users without degrading overall performance.

- **The price of robustness (cost of the proposed service system design).** Robustness refers to the ability of a service system to sustain acceptable performance under demand variability and adverse operating conditions. The *price of robustness* measures the additional cost required to transition from the current estimated configuration to a design that delivers improved stability, lower congestion, and reduced tail risk. Since implementation decisions ultimately depend on budget considerations, quantifying this cost is essential for assessing the practical viability of the proposed framework.

Figure ?? (right panel) reports borough-level cost deviations, expressed as percentages relative to the current system. Cost increases are not uniform across boroughs: high-demand areas require larger adjustments, reflecting the need for additional capacity to prevent persistent saturation. However, all increases remain within the same order of magnitude, indicating that robustness is achieved through coordinated system-level redesign rather than localized overprovisioning.

A similar pattern emerges across operational profiles (see Appendix D). Profiles emphasizing strict guarantees or tail protection entail higher cost increments, as expected, since reducing extreme delays requires structural slack. In contrast, balanced or efficiency-oriented profiles exhibit more moderate cost adjustments.

The congestion- and tail-aware system architecture leads to an increase of up to 300% in every borough and ranges from 150% to over 600% across the different profiles. Nevertheless, such deviation might be readily tailored when decision-making is driven by the effective cost considerations. Note that suitable smaller values of parameter κ make the loss function (8) prioritizes the cost, being able to reach the most conservative service capacity while still keep the quality requirements when κ equals zero. On the contrary, larger values of κ prevail the emphasis on reducing congestion levels. The motivations behind the decision-making process and the state of nature are captured within this flexible modeling framework, enabling the system to achieve proper equilibrium. The evidence shows that substantial gains in efficiency, congestion control, and fairness can be achieved at a measurable and economically interpretable cost, supporting informed adoption in real urban service systems.

5. CONCLUSION

We develop an optimization-based framework for the design of multi-regime parallel service queueing systems under congestion and risk considerations. The core contribution is a flexible mixed-integer exponential conic formulation that integrates (i) service-level agreement (SLA) chance constraints protecting a prescribed fraction of users, (ii) structural design constraints modeled through conflict graphs, and (iii) explicit tail-risk control under the CVaR paradigm.

Although the resulting problem is NP-hard, we design an efficient decomposition approach that substantially alleviates the computational burden in large-scale instances. Moreover, we

show that under suitable structural simplifications, a constructive polynomial-time procedure can be derived, thereby identifying tractable regimes of the model and clarifying the boundary between complexity and structure.

From a practical standpoint, the framework provides a unified decision-support tool for service system design. The case study demonstrates that the optimized design delivers substantial and systematic improvements in efficiency, congestion control, fairness, and robustness. In particular, the “prices of” efficiency, congestion control, fairness, and robustness are shown to be measurable and transparent, allowing decision makers to explicitly quantify trade-offs between response time reduction, system stability, tail-risk mitigation, and budgetary adjustments.

Overall, the proposed methodology bridges modern conic optimization modeling with actionable service system design, offering both theoretical insight and operational value for large-scale urban service applications.

A natural avenue for future research is the extension of the framework to multi-facility service systems in which assignment decisions endogenously determine arrival rates. In such settings, allocation policies would interact with congestion dynamics, leading to joint design and routing models with coupled arrival and service mechanisms.

ACKNOWLEDGEMENTS

The authors acknowledge financial support by grants PID2020-114594GB-C21, PID2022-139219OB-I00, PID2024-156594NB-C21, and RED2022-134149-T (Thematic Network on Location Science and Related Problems) funded by MICIU/AEI/10.13039/501100011033; FEDER+Junta de Andalucía projects C-EXP-139-UGR23, and AT 21_00032; SOL2024-31596 and SOL2024-31708 funded by US; the IMAG-Maria de Maeztu grant CEX2020-001105-M / AEI / 10.13039 / 501100011033; and the IMUS-Maria de Maeztu grant CEX2024-001517-M.

APPENDIX A. SSD(C/TR)-ECP FULL MODEL

$$\begin{aligned} \min \quad & c^t \mu - \kappa \sum_{r \in \mathcal{R}} \nu_r && \text{SSD(C/TR)-ECP} \\ \text{s.t.} \quad & \mu_r - \Lambda_r \geq \varepsilon, && \forall r \in \mathcal{R}, \end{aligned} \tag{17}$$

$$\begin{aligned} & \sum_{r \in \mathcal{R}} \pi_r \zeta_{ar} \leq 1 + (\alpha_a - 1)s_a, && \forall a \in \mathcal{A}, \\ & u_{ar} = -(\mu_r - \Lambda_r)(t_a^* - t_a), && \forall a \in \mathcal{A}, r \in \mathcal{R}, \\ & (\zeta_{ar}, s_a, u_{ar}) \in \mathcal{K}_{\text{exp}}, && \forall a \in \mathcal{A}, \forall r \in \mathcal{R}, \end{aligned} \tag{18}$$

$$\begin{aligned} & \sum_{a \in \mathcal{A}} s_a \geq \lceil \beta |\mathcal{A}| \rceil, \\ & s_a + s_{a'} \leq 1, && \forall \{a, a'\} \in \mathcal{E}, \end{aligned} \tag{19}$$

$$r_a \geq t_a + \sum_{r \in \mathcal{R}} \pi_r \tau_r, \quad \forall a \in \mathcal{A}, \tag{20}$$

$$\eta + \frac{\sum_{a \in \mathcal{A}} U_a}{\lfloor (1 - \gamma) |\mathcal{A}| \rfloor} \leq \Gamma, \tag{21}$$

$$\nu_r + \ell_r \geq 0, \quad \forall r \in \mathcal{R}, \tag{22}$$

$$(\tau_r, 1, \ell_r) \in \mathcal{K}_{\text{exp}}, \quad \forall r \in \mathcal{R}, \tag{23}$$

$$(\mu_r - \Lambda_r, 1, \nu_r) \in \mathcal{K}_{\text{exp}}, \quad \forall r \in \mathcal{R}, \tag{24}$$

$$\mu_r, \nu_r, \ell_r, \tau_r \geq 0, \quad \forall r \in \mathcal{R},$$

$$U_a, r_a \geq 0, \quad \forall a \in \mathcal{A},$$

$$\eta \geq 0,$$

$$s_a \in \{0, 1\}, \quad \forall a \in \mathcal{A}.$$

APPENDIX B. BENDERS DECOMPOSITION FOR SSD(C/TR)-ECP

This appendix provides the detailed derivation of the Benders decomposition used to solve problem **SSD(C/TR)-ECP**.

Fixing $s = \bar{s} \in \{0, 1\}^{\mathcal{A}}$, the continuous subproblem defining $\Theta(\bar{s})$ is given by

$$\begin{aligned}
\min \quad & c^t \mu - \kappa \sum_{r \in \mathcal{R}} \nu_r \\
\text{s.t.} \quad & (17), (18), (19) - (24), \\
& \sum_{r \in \mathcal{R}} \pi_r \zeta_{ar} \leq 1 + (\alpha_a - 1) \bar{s}_a, \quad \forall a \in \mathcal{A}, \quad (25) \\
& (\zeta_{ar}, \bar{s}_a, u_{ar}) \in \mathcal{K}_{\text{exp}}, \quad \forall a \in \mathcal{A}, \forall r \in \mathcal{R}, \quad (26) \\
& \bar{s}_a + \bar{s}_{a'} \leq 1, \quad \forall \{a, a'\} \in \mathcal{E}, \quad (27) \\
& \mu_r, \nu_r, \ell_r, \tau_r \geq 0, \quad \forall r \in \mathcal{R}, \\
& U_a, r_a \geq 0, \quad \forall a \in \mathcal{A}, \\
& \eta \geq 0,
\end{aligned}$$

Note that all constraints in the problem above are convex. Thus, assuming that the subproblem is feasible, and since the problem clearly verifies strong duality (e.g., by Slater's condition), let $f_a, g_{\{a, a'\}} \geq 0$ denote the dual multipliers associated with (25) and (27), respectively, and let

$$h_{ar} = (h_{ar}^{(1)}, h_{ar}^{(2)}, h_{ar}^{(3)}) \in \mathcal{K}_{\text{exp}}^*$$

be the dual vector associated with (26). The second component $h_{ar}^{(2)}$ corresponds to the coordinate in which \bar{s}_a appears. Collecting the terms of the Lagrangian that depend on \bar{s} , we obtain

$$\sum_{a \in \mathcal{A}} (1 - \alpha_a) f_a \bar{s}_a + \sum_{\{a, a'\} \in \mathcal{E}} g_{\{a, a'\}} (\bar{s}_a + \bar{s}_{a'}) + \sum_{a \in \mathcal{A}} \sum_{r \in \mathcal{R}} h_{ar}^{(2)} \bar{s}_a.$$

Therefore, a subgradient of $\Theta(\cdot)$ at \bar{s} is given componentwise by

$$q_a(\bar{s}) = (1 - \alpha_a) f_a + \sum_{e \in \mathcal{E}: a \in e} g_e + \sum_{r \in \mathcal{R}} h_{ar}^{(2)},$$

for all $a \in \mathcal{A}$. By convexity of $\Theta(\cdot)$, the supporting hyperplane inequality yields,

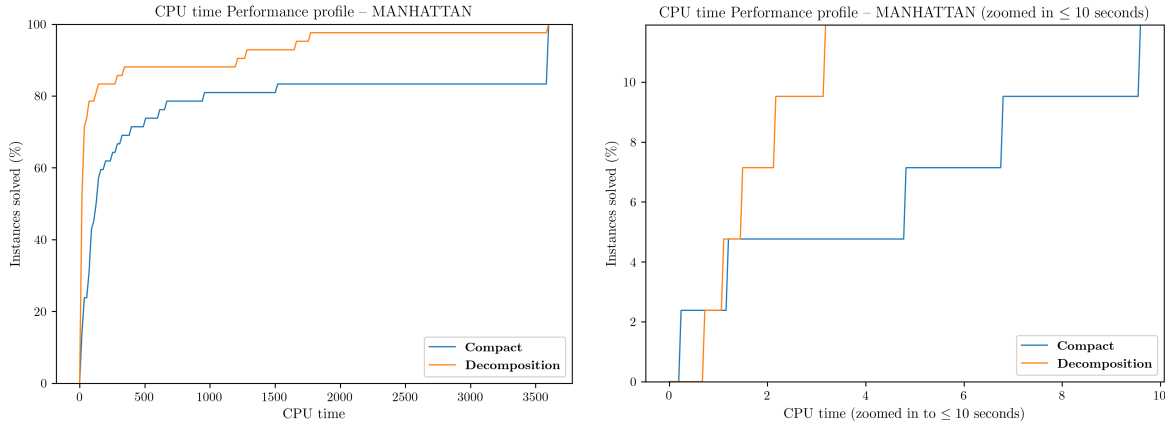
$$\Theta(s) \geq \Theta(\bar{s}) + \sum_{a \in \mathcal{A}} q_a(\bar{s})(s_a - \bar{s}_a), \quad \forall s \in [0, 1]^{\mathcal{A}}.$$

Introducing the master variable θ , this inequality gives rise to the Benders optimality cut

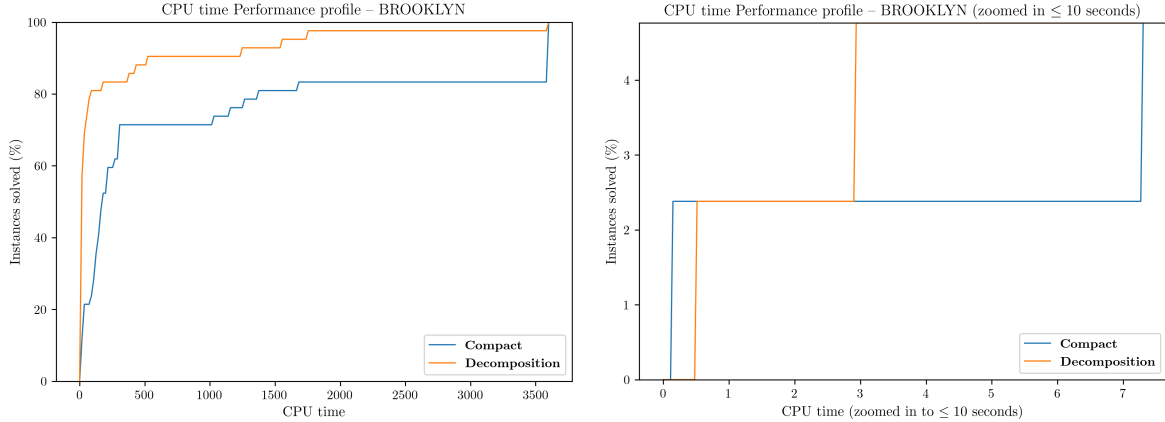
$$\theta \geq \Theta(\bar{s}) + \sum_{a \in \mathcal{A}} q_a(\bar{s})(s_a - \bar{s}_a).$$

If the subproblem is infeasible for \bar{s} , a feasibility cut excluding this solution is added

$$\sum_{a \in \mathcal{A}: \bar{s}_a = 1} s_a \leq |\{a \in \mathcal{A} : \bar{s}_a = 1\}| - 1.$$



Performance Profile of CPU Time for Manhattan in our experiments (left) and zoomed to those solved in less than 10 seconds (right).



Performance Profile of CPU Time for Brooklyn in our experiments (left) and zoomed to those solved in less than 10 seconds (right).

APPENDIX C. COMPUTATIONAL PERFORMANCE. ADDITIONAL PLOTS

APPENDIX D. CASE STUDY. ADDITIONAL PLOTS

REFERENCES

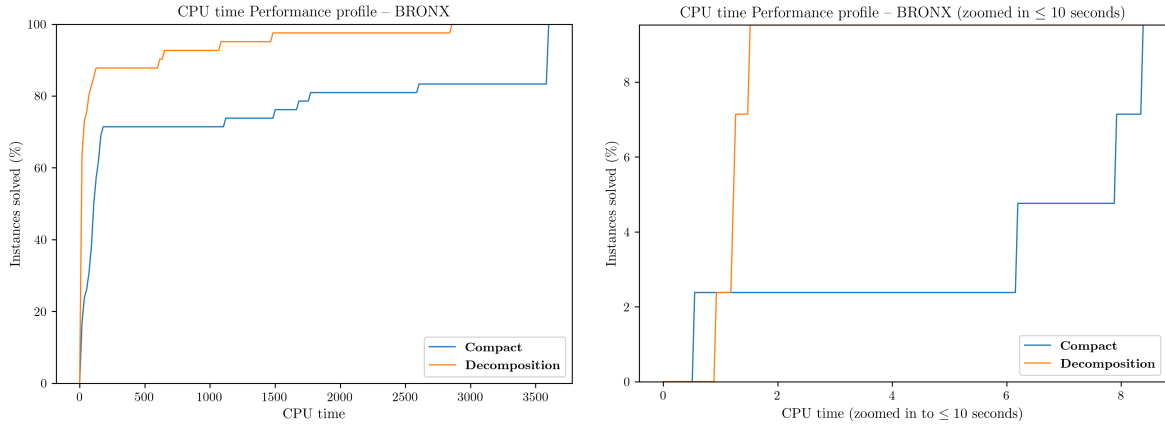
Robert Aboolian, Oded Berman, and Zvi Drezner. Location and allocation of service units on a congested network. *IIE Transactions*, 40(4):422–433, 2008.

Robert Aboolian, Oded Berman, and Majid Karimi. Probabilistic set covering location problem in congested networks. *Transportation Science*, 56(2):528–542, 2022a.

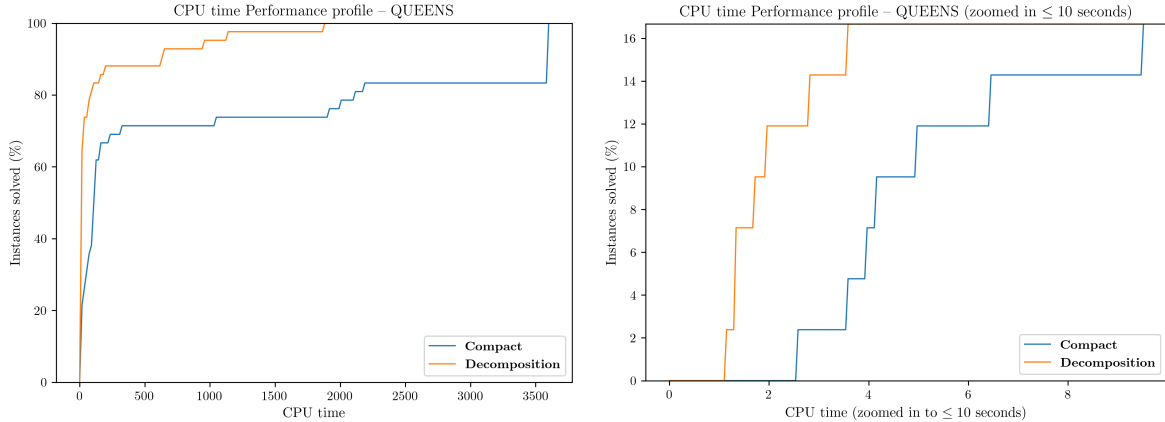
Robert Aboolian, Samir Elhedhli, and Majid Karimi. An efficient approach for service system design with immobile servers, stochastic demand, congestion, and consumer choice. *Journal of Supply Chain and Operations Management*, 20(1):1–18, 2022b.

Søren Asmussen. *Applied Probability and Queues*. Springer, 2nd edition, 2003.

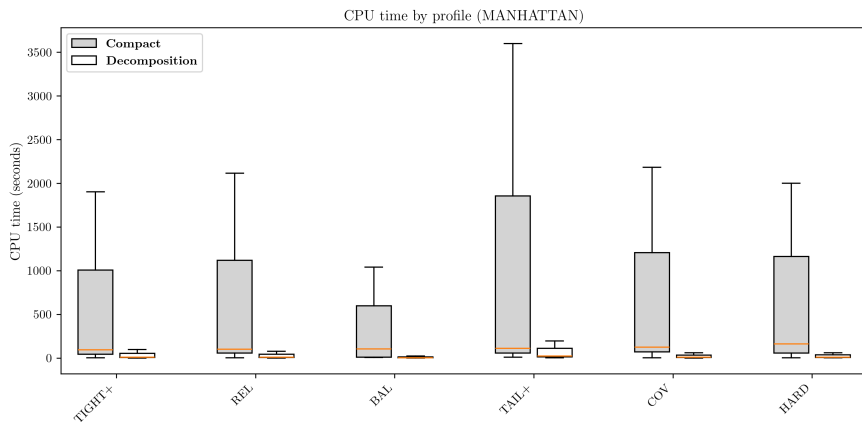
Aharon Ben-Tal and Arkadi Nemirovski. *Lectures on Modern Convex Optimization: Analysis, Algorithms, and Engineering Applications*. SIAM, 2001.



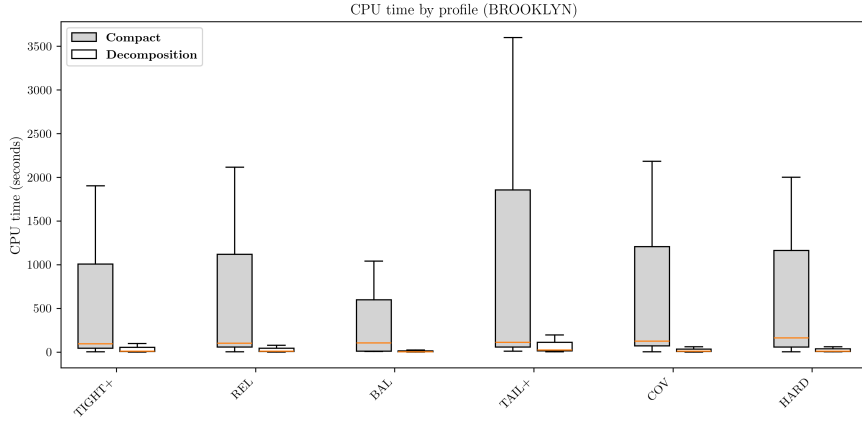
Performance Profile of CPU Time for Bronx in our experiments (left) and zoomed to those solved in less than 10 seconds (right).



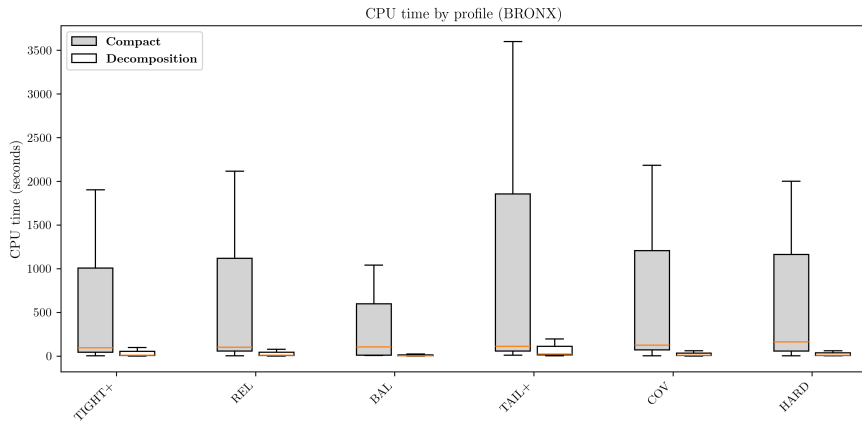
Performance Profile of CPU Time for Queens in our experiments (left) and zoomed to those solved in less than 10 seconds (right).



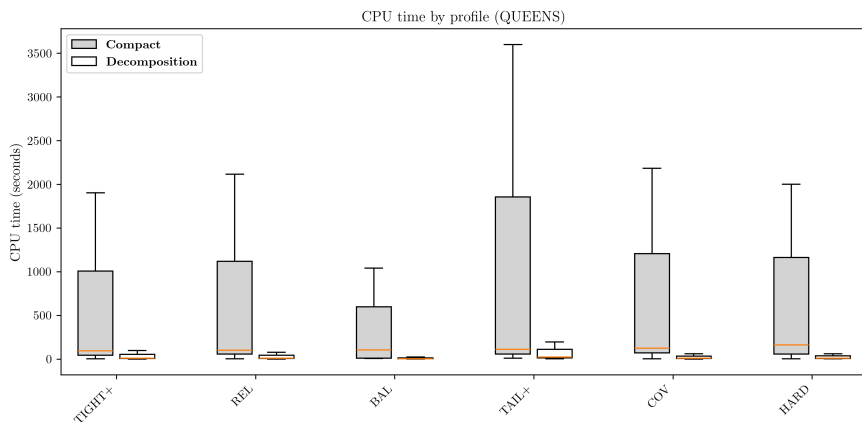
Boxplots of CPU time by profile for Manhattan. For each profile, the distribution of CPU times is shown for the **compact** and **decomposition** approaches.



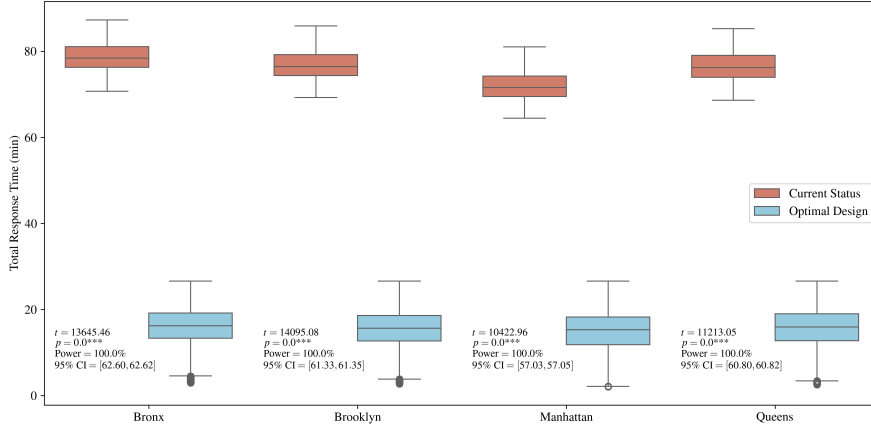
Boxplots of CPU time by profile for Brooklyn. For each profile, the distribution of CPU times is shown for the **compact** and **decomposition** approaches.



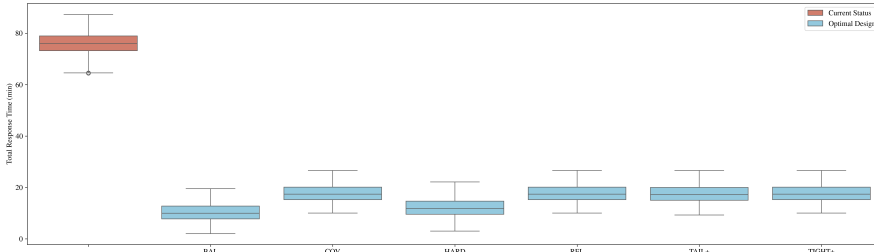
Boxplots of CPU time by profile for Bronx. For each profile, the distribution of CPU times is shown for the **compact** and **decomposition** approaches.



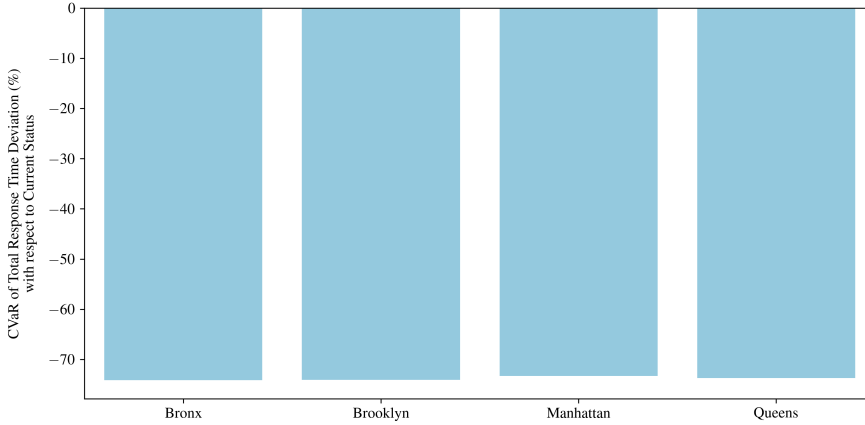
Boxplots of CPU time by profile for Queens. For each profile, the distribution of CPU times is shown for the **compact** and **decomposition** approaches.



Boxplots of obtained response times with the estimated rates and those obtained with our models for each borough.



Boxplots of obtained response times with the estimated rates and those obtained with our models for each parameters profile.

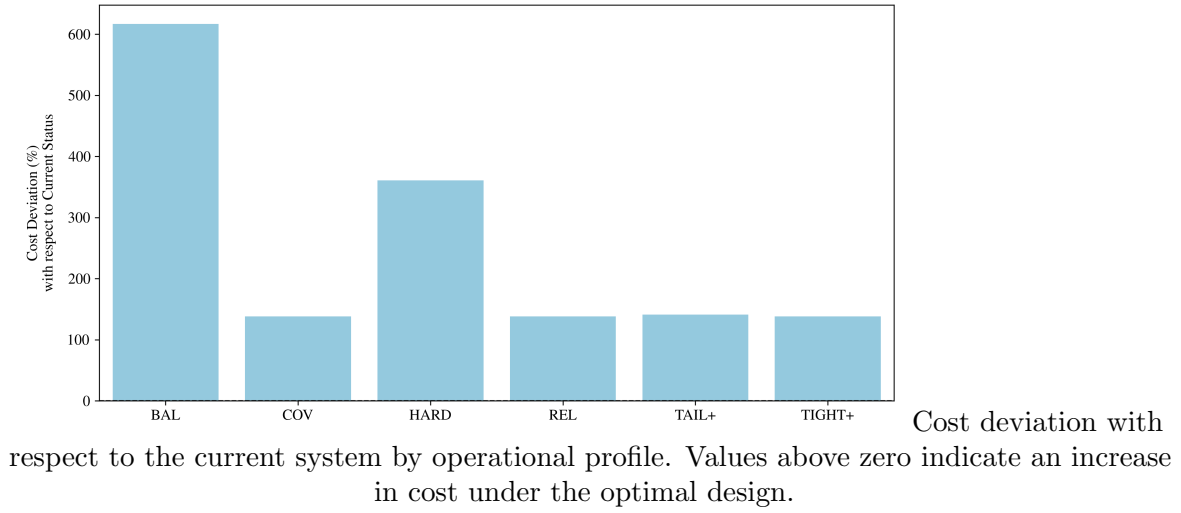
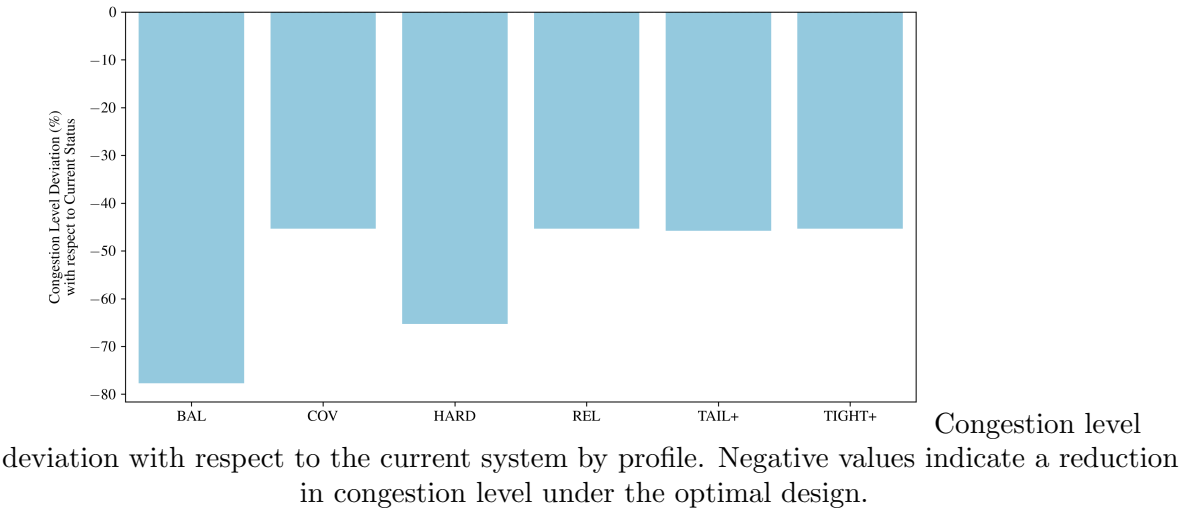
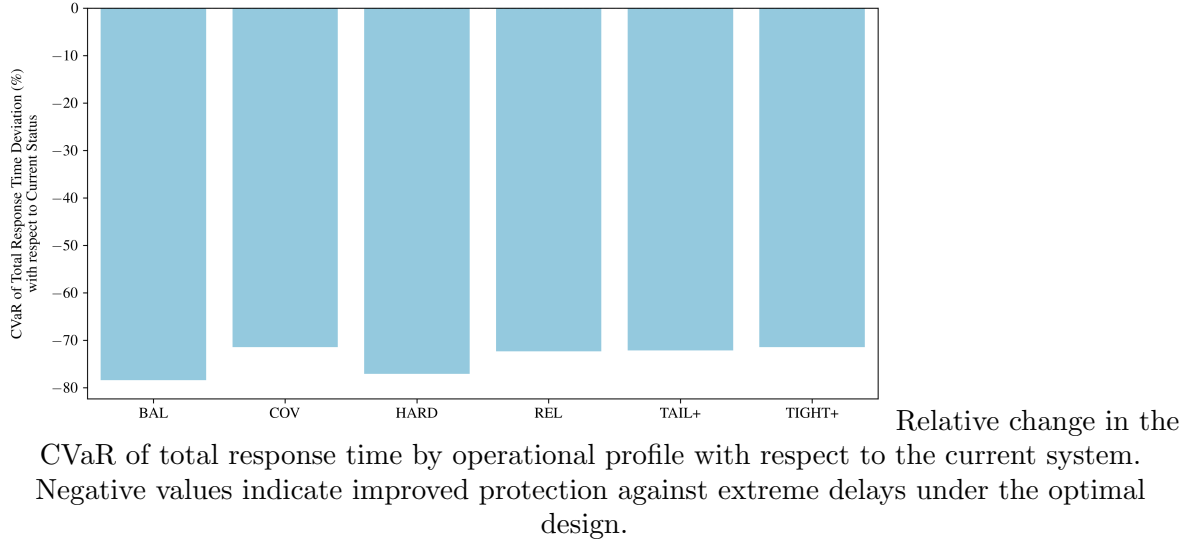


Relative change in the CVaR of total response time by borough with respect to the current system. Negative values indicate a reduction in extreme response times under the optimal design.

Oded Berman, Richard C. Larson, and Shih-Fen Chiu. Optimal server location on a network operating as an M/G/1 queue. *Operations Research*, 33(4):746–759, 1985.

Oded Berman, Dmitry Krass, and Michael B.C. Menezes. Location problems with congestion. *Annals of Operations Research*, 111(1):97–113, 2003.

Dimitris Bertsimas and Melvyn Sim. The price of robustness. *Operations research*, 52(1):35–53, 2004.



Dimitris Bertsimas, Vishal Gupta, and Nathan Kallus. Fairness constraints in optimization. *Operations Research*, 66(3):608–628, 2018.

Sem C. Borst, Avishai Mandelbaum, and Martin I. Reiman. Dimensioning large call centers. *Operations Research*, 52(1):17–34, 2004.

Stephen Boyd and Lieven Vandenberghe. *Convex Optimization*. Cambridge University Press, 2004.

René Caldentey, Lisa Aoki Hillas, and Varun Gupta. Designing service menus for bipartite queueing systems. *Operations Research*, 73(3):1496–1534, 2025.

Francesco Cesarone and Justo Puerto. Flexible enhanced indexation models through stochastic dominance and ordered weighted average optimization. *European Journal of Operational Research*, 323(2):657–670, 2025.

Pablo Chares. *Cones and Interior-Point Algorithms for Structured Convex Optimization*. PhD thesis, University of California, Los Angeles, 2009.

Feng Cheng and Jiazhen Huo. The staffing requirements with time-varying demand and customer abandonment in call centers. *Innovation and Supply Chain Management*, 7(1):19–24, 2013.

Mark S. Daskin. *Network and Discrete Location: Models, Algorithms, and Applications*. Wiley, 2013.

Michal Feldman and Tami Tamir. Conflicting congestion effects in resource allocation games. *Operations research*, 60(3):529–540, 2012.

Anja Feldmann and Ward Whitt. Fitting mixtures of exponentials to long-tail distributions. *Performance Evaluation*, 31(3–4):245–279, 1998.

Michael R Garey and David S Johnson. *Computers and Intractability*, volume 29. New York: wh freeman, 2002.

O. Garnett, A. Mandelbaum, and M. Reiman. Designing a call center with impatient customers. *Manufacturing & Service Operations Management*, 5(4):335–353, 2002.

Julio C Gómez and Miguel F Anjos. Second-order cone optimization formulations for service system design problems with congestion. In *Modeling and Optimization: Theory and Applications*, pages 97–120. Springer, 2017.

Donald Gross, John F. Shortle, James M. Thompson, and Carl M. Harris. *Fundamentals of Queueing Theory*. John Wiley & Sons, 4th edition, 2008.

Itai Gurvich and Ward Whitt. Queue-and-idleness-ratio controls in many-server service systems. *Mathematics of Operations Research*, 34(2):363–396, 2009.

Mor Harchol-Balter. *Performance Modeling and Design of Computer Systems*. Cambridge University Press, 2013.

J. Michael Harrison and Assaf Zeevi. A method for staffing large call centers based on stochastic fluid models. *Manufacturing & Service Operations Management*, 7(1):20–36, 2005.

Refael Hassin and Moshe Haviv. *To Queue or Not to Queue: Equilibrium Behavior in Queueing Systems*. Springer Science & Business Media, Boston, MA, 2003. ISBN 978-1-4615-0359-0. doi: 10.1007/978-1-4615-0359-0.

Per Hokstad. Approximations for the M/G/m queue. *Operations Research*, 26(3):510–523, 1978.

Gaurav Jain, Deepali Singh, and Shekhar Verma. Service level agreements in IP networks. *Information Management & Computer Security*, 10(4):171–177, 2002.

Leonard Kleinrock. *Queueing Systems, Volume I: Theory*. Wiley, 1975.

Zhenghua Long, Hailun Zhang, Jiheng Zhang, and Zhe George Zhang. The generalized c/μ rule for queues with heterogeneous server pools. *Operations Research*, 72(6):2488–2506,

2024.

ApS Mosek. *The MOSEK Python Fusion API manual. Version 11.0.*, 2025. URL <https://docs.mosek.com/latest/pythonfusion/index.html>.

Włodzimierz Ogryczak and Arie Tamir. Minimizing the sum of the k largest functions in linear time. *Information Processing Letters*, 85(3):117–122, 2003.

Justo Puerto, Antonio M Rodríguez-Chía, and Arie Tamir. Revisiting k -sum optimization. *Mathematical Programming*, 165(2):579–604, 2017.

R. Tyrrell Rockafellar and Stanislav Uryasev. Optimization of conditional value-at-risk. *Journal of Risk*, 2(3):21–41, 2000.

R. Tyrrell Rockafellar and Stanislav Uryasev. Conditional value-at-risk for general loss distributions. *Journal of Banking & Finance*, 26(7):1443–1471, 2002.

Seung Bum Soh and Itai Gurvich. Call center staffing: Service-level constraints and index priorities. *Operations Research*, 65(2):537–555, 2017.

John N Tsitsiklis and Kuang Xu. Flexible queueing architectures. *Operations Research*, 65(5):1398–1413, 2017.

Ronald W. Wolff. *Stochastic Modeling and the Theory of Queues*. Prentice Hall, 1989.

Noa Zychlinski, Carri W Chan, and Jing Dong. Managing queues with different resource requirements. *Operations Research*, 71(4):1387–1413, 2023.